4-2-2021

Polymer particles for the intra-articular delivery of drugs to treat osteoarthritis

Xueli Mei
The University of Western Ontario

Ian J. Villamagna
The University of Western Ontario

Tony Nguyen
The University of Western Ontario

Frank Beier
The University of Western Ontario

C. Thomas Appleton
The University of Western Ontario

See next page for additional authors

Polymer Particles for the Intra-articular Delivery of Drugs to Treat Osteoarthritis

Xueli Mei,[1] Ian J. Villamagna,[2,3] Tony Nguyen,[1] Frank Beier,[3,4] C. Thomas Appleton,[3,4,5] Elizabeth R. Gillies*[1,2,3,6]

*Author to whom correspondence should be addressed: egillie@uwo.ca

[1] Department of Chemistry, The University of Western Ontario, 1151 Richmond St., London, Ontario, Canada, N6A 5B7

[2] School of Biomedical Engineering, The University of Western Ontario, 1151 Richmond St., London, Ontario, Canada, N6A 5B9

[3] Bone and Joint Institute, The University of Western Ontario

[4] Department of Physiology and Pharmacology, The University of Western Ontario, 1151 Richmond St., London, Ontario, Canada, N6A 3B7

[5] Department of Medicine, The University of Western Ontario, 1151 Richmond St., London, Ontario, Canada, N6A 5C1

[6] Department of Chemical and Biochemical Engineering, The University of Western Ontario, 1151 Richmond St., London, Ontario, Canada, N6A 5B9

Abstract

Osteoarthritis (OA) is a leading cause of chronic disability. It is a progressive disease, involving pathological changes to the entire joint, resulting in joint pain, stiffness, swelling, and loss of mobility. There is currently no disease-modifying pharmaceutical treatment for OA, and the treatments that do exist suffer from significant side effects. An increasing understanding of the molecular pathways involved in OA is leading to many potential drug targets. However, both current and new therapies can benefit from a targeted approach that delivers drugs selectively to joints at therapeutic concentrations, while limiting systemic exposure to the drugs. Delivery systems including hydrogels, liposomes, and various types of particles have been explored for intra-articular drug delivery. This review will describe progress over the past several years in the development of polymer-based particles for OA treatment, as well as their *in vitro*, *in vivo*, and clinical evaluation. Systems based on biopolymers such as polysaccharides and polypeptides, as well as synthetic polyesters, poly(ester amide)s, thermoresponsive polymers, poly(vinyl alcohol), amphiphilic polymers, and dendrimers will be described. We will discuss the role of particle size, biodegradability, and mechanical properties in the behavior of the particles in the joint, and the challenges to be addressed in future research.

Keywords

Osteoarthritis, drug delivery, intra-articular, nanoparticle, microparticle, polymer

1. Introduction

Osteoarthritis (OA) is the most common type of arthritis, affecting more than 240 million people worldwide [1, 2]. It is a leading cause of global disability [3]. The prevalence of OA has been continually increasing over the past several decades due to increasing risk factors such as an aging population, growing obesity rates, and other contributors [4]. The socioeconomic burden associated with pain and loss of function from OA is large, costing between 1 and 2.5% of gross domestic product in developed countries [5]. Furthermore, OA is a significant risk factor for many other diseases such as cardiovascular and metabolic diseases and depression.

OA is a progressive disease of the entire joint, with alterations leading to overall degeneration of the joint, resulting in joint pain, stiffness, swelling, and reduced mobility (**Figure 1**). The two bones that make up a synovial joint are covered with articular cartilage. When healthy, articular cartilage has a smooth surface that exhibits a low coefficient of friction, allowing the bones to move freely and smoothly [6]. It is viscoelastic and designed to distribute loads across the joint evenly. Chondrocytes, the cells within cartilage, produce extracellular matrix (ECM), consisting primarily of collagen type 2 and proteoglycans [7]. The cartilage is often considered to be one of the most altered tissues in OA, undergoing thinning and damage [8], due to an increase in catabolic factors such as matrix metalloproteinases (MMPs) and a decrease in anabolic factors [9]. Subchondral bone forms an interface between cartilage and the trabecular bone [10]. It plays an important role in the function of the joint, acting as a shock absorber [11], and supplying the joint with nutrients to maintain homeostasis [10]. In this context, damage to the bone can cause major metabolic changes in cartilage [12]. In early progression of OA, the interface between the subchondral bone and articular cartilage undergoes distinct remodeling, especially in areas where cartilage damage is present [13]. As OA progresses, a decrease in mineralization and reduced bone stiffness are noted.

The synovial membrane is a soft tissue that lines synovial joints, serving as a barrier to the joint space [14]. To retain synovial fluid, the intimal layer of the synovial membrane exhibits a free exchange of proteins and molecules, while inhibiting the transit of the hyaluronic acid (HA), which is an important component of the joint fluid. The synovial membrane also plays an integral role in the lubrication of cartilage through the secretion of the proteoglycan lubricin as well as molecules that are imperative for the nutrition of the joint cells and tissues. In OA, the most common change in the synovial membrane involves the inflammation and enlargement of the tissue, known as synovitis, which is believed to be a major driving factor behind the pain associated with OA [15]. It has been hypothesized that as cartilage begins to break down as a result of OA, the byproducts are released into the synovial fluid, which are then phagocytosed by synovial macrophages. The inflamed synovial membrane then further produces catabolic and pro-inflammatory cytokines, leading to a production of enzymes which break down the cartilage further. The synovial fluid is a viscous solution that is an important component of the joint [16]. HA and lubricin in synovial fluid function to reduce the friction between the articular cartilage of the joint during movement. HA also plays an important role in cartilage protection and nutrient

transport to cartilage. In OA, there is a marked increase in catabolic and pro-inflammatory cytokines in the synovial fluid. In addition, the level of proteins and overall volume of synovial fluid increase, which can lead to further inflammation of the joint [16].

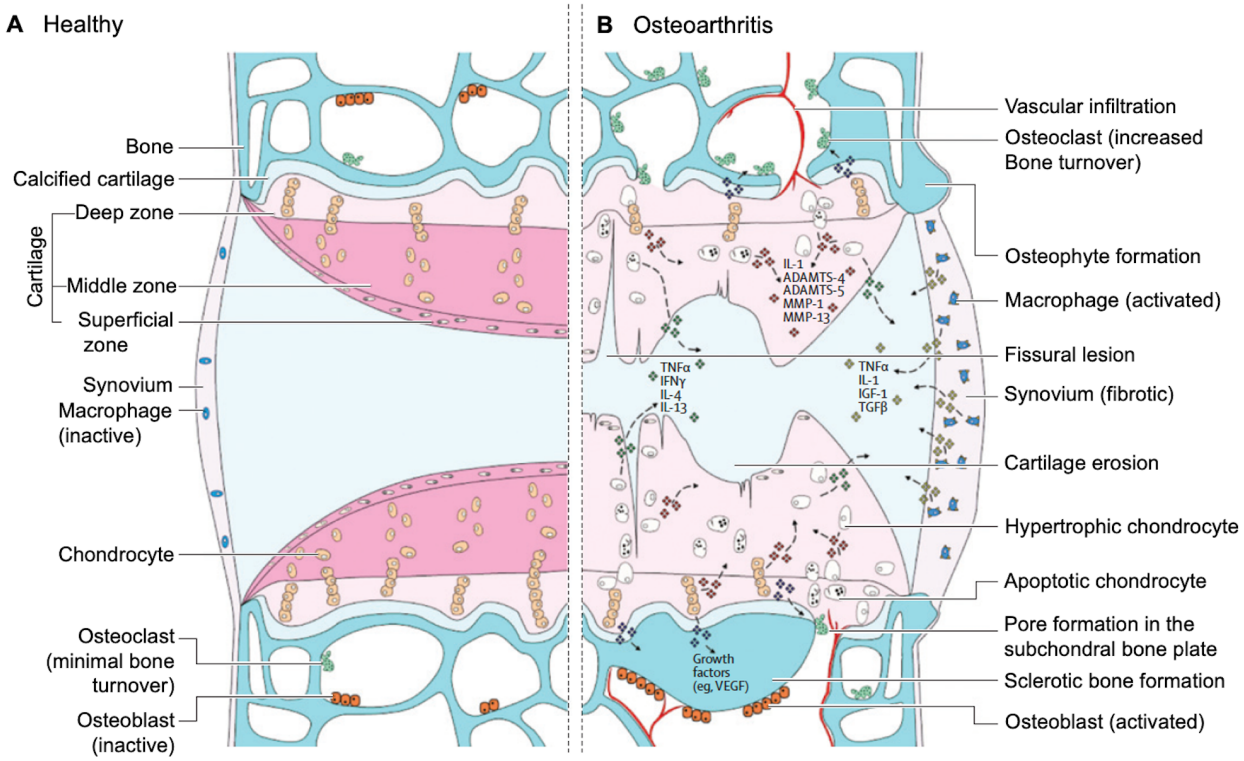

Figure 1. Structural changes and biochemical signaling in OA development. IL = interleukin; IGF = insulin-like growth factor; IFN = interferon; TNF = tumor necrosis factor; VEGF = vascular endothelial growth factor; ADAMTS = a disintegrin and metalloproteinase with thrombospondin-like motifs; TGF = transforming growth factor. Reproduced from reference [6] with permission from Elsevier.

Despite the prevalence of OA and a growing understanding of the mechanisms underlying disease progression, there are currently no disease-modifying drugs to treat OA. Evidence-based treatment is therefore aimed at improving symptoms and function [17]. Treatment of OA remains variable from patient to patient and is tailored to the progression and the stage of the disease, as well as patient preferences. Of the current non-pharmacologic treatments for OA, exercise and weight loss have been shown to lead to beneficial effects [18, 19]. Oral medications, such as acetaminophen, or non-steroidal anti-inflammatory drugs

(NSAIDs) such as celecoxib (CXB) and meloxicam are also frequently used [20]. While effective in mitigating pain and stiffness, cardiovascular, gastrointestinal, and renal risks often limit the effective use of NSAIDs [21]. Topical NSAIDs and other ointments have been developed as safer alternatives to oral medications, as they can be applied selectively in proximity to the affected joint, leading to a lower systemic dose [22], but their clinical benefits remain unclear [20, 23]. To increase the availability of drug in the joint, intra-articular (IA) injections are used [24]. Methylprednisolone, triamcinolone and dexamethasone (DEX) are steroids that have commonly been injected for the treatment of OA [25]. However, they provide only short-term relief and concerns have been raised regarding their potentially detrimental effects on cartilage [26, 27]. Viscosupplementation is a means of replacing naturally occurring lubricating molecules within the joint that are either damaged or lost when OA progresses. These injections typically contain HA, HA derivatives, or chondroitin sulfate (CS) [20]. Their clinical efficacy remains questioned [28]. Depending on the joint affected, the response to the aforementioned therapies, and other patient specific factors, total joint replacement therapy can be performed to treat refractory symptoms in late-stage OA [29]. This surgery provides relief for many patients, but has shortcomings including lack of efficacy in some patients, risk of infections during or after surgery, high cost, limited lifespan of implants, especially when implanted in mid-life, and altered biomechanics that can cause degenerative changes in other parts of the body [6].

There is an undeniable need to develop disease-modifying agents that can alter the progression of OA, rather than solely treat its symptoms. The molecular pathways involved in the onset and progression of OA have been studied intensively in recent years, leading to the proposal of potential disease-modifying drugs [30]. As the loss of articular cartilage is a hallmark of OA, cartilage is a key therapeutic target. Inhibition of MMPs, which degrade collagen, has been pursued with inhibitors such as PG-116800, but dose-dependent adverse effects have been observed [31]. Inhibitors of the aggrecanase ADAMTS5 were recently evaluated in a Phase 2 clinical trial but failed in all endpoints [32, 33]. Anti-ADAMTS5 antibodies are also under study [34]. In addition, molecules capable of promoting cartilage repair have also been investigated. For example, recombinant human fibroblast growth factor (FGF)18 (sprifermin) was recently shown in Phase 2 clinical trials to reduce cartilage loss, though it did not lead to improvements in clinical symptoms [35]. The delivery of TGFβ via IA injection of allogenic chondrocytes is also

under investigation [36]. The cathepsin K inhibitor MIV-711, that targets the bone remodeling associated with OA, has also been investigated in clinical trials [37]. It was found to reduce cartilage thinning and reduce changes in bone that are associated with OA, but was not effective in reducing pain.

Inflammation can lead to pain and degradation of the joint tissues [38]. A number of studies have focused on controlling inflammatory signaling cascades through the control of cytokines associated with OA [12]. IL-1β is a common target. Anakinra is an IL-1 receptor antagonist but has seen mixed results in clinical trials [39]. TNFα was also identified as a major proinflammatory cytokine associated with OA [12]. However, the clinical efficacy of TNFα inhibitors has not yet been demonstrated [40]. Nuclear factor-κB (NF-κB) is integral to the production of pro-inflammatory cytokines, and its inhibition has been targeted using SAR113945. Beneficial effects were observed in phase I trials but phase II trials failed to demonstrate similar responses [41]. P38 mitogen activated protein kinase (MAPK) is another potential target associated with the synthesis of pro-inflammatory cytokines which is under investigation [42]. Activation of peroxisome proliferator-activated receptor (PPAR)δ has been implicated in the degradation of cartilage ECM, suggesting PPARδ inhibition as a potential therapeutic strategy [43]. Although pain is also considered a symptom of OA, the synergistic relationships between the pain mechanisms, inflammation, and structural alteration within the joint have been demonstrated [30]. The TRP Vanilloid 1 (TRPV1) receptor is the target of CNTX-4975 [44], which advanced into phase IIb clinical trials, showing a reduction in pain over 24 weeks. However, negative side effects and potential safety concerns with TRPV1 antagonists have been noted [45]. Nerve growth factor (NGF) is a neuropeptide implicated in enhanced perception of pain and a triggering of the initial pain response in OA. Monoclonal antibodies to NGF were deemed promising in preclinical studies, but safety concerns became quickly apparent in clinical trials [46].

IA drug delivery is increasingly recognized as a promising strategy for the administration of OA drugs. Compared with systemic administration, IA injections can potentially deliver the right dose of drug to the target tissue, while greatly reducing systemic exposure to the drug [47]. IA delivery may therefore mitigate the adverse side effects that are problematic for many potential OA therapeutics. However, free drugs are removed from the IA space by capillaries and

the lymphatics within a few hours [48]. In addition, the frequency of IA injections should be minimized, ideally to once every 3 months or less frequent [49, 50]. The rapid clearance of drugs from the joint, combined with a limited frequency of treatment, may be contributing to the failure of some potential therapeutics to achieve clinical benefits in trials. Therefore, many drugs would benefit from incorporation into delivery systems that provide sustained release.

A number of delivery systems have been explored for the IA delivery of OA drugs. For example, hydrogels based on HA [51], elastin-like peptides [52], and poly(caprolactone-*co*-lactide)(PCLA)-poly(ethylene glycol)(PEG)-PCLA [53, 54] have been investigated. Liposomes have also been explored [42, 55]. This review will focus on delivery systems based on polymeric particles. We will discuss both biopolymer and synthetic polymer systems and will focus on developments over the past five years, as earlier systems have already been described in previous review articles [56-61] (Table 1). Nanoparticles are typically defined as having at least one dimension (e.g., diameter) between 1 and 100 nm, while microparticles are considered to have dimensions between 1 and 1000 μm. In practice, either term has been used for materials with intermediate dimensions (i.e., 100 nm – 1 μm). Given the importance of particle size in determining factors such as cellular uptake, clearance, and trafficking *in vivo*, we will include both nanoparticles and microparticles in this review and will discuss the effects of particle size on their behavior in the joint. Finally, we will conclude with some challenges and perspectives for future work in the field.

Table 1. Summary of the polymers, drugs, and characteristics of the different particle-based delivery systems discussed in this review. NR = not reported.

Polymer	**Therapeutic incorporated**	**Particle diameter**	**Drug release time (*in vitro*)**	**In vivo results**
Chitosan	Lornoxicam [70]	3.6 – 6.1 μm	8 days	Reduced inflammation and histopathological markers of OA in rats
	Sinomenium [71]	100 μm	96 h	Reduced cartilage degradation and slowed OA progression in mice
	KGN [74]	150 nm, 1.8 μm	50 – 50% over 7 weeks	Reduced cartilage damage and OARSI score in rats
	KGN and DCF [77]	350 – 650 nm	20 – 50% over 14 days (kartogenin) 20 – 90% over 24 h (diclofenac)	Particles retained in rat joints for 14 days; Reduced OA progression
	Berberine [78]	50 – 400 nm	70% over 7 days	Cartilage protective effect in rats
	Clodronate [80]	146 nm	90% over 48 h	NR
	CrmA DNA [83]	50 nm	60% over 7 days	Reduced cartilage degradation, mRNA of MMPs and IL-1β in rabbits
HA	Glucosamine [87]	175 – 187 nm	20% over 21 days	NR
	CXB [90]	250 – 450 nm	7 days	Reduced swelling and cartilage damage in rats
HA-chitosan	Curcuminoid [91]	165 nm	74% over 72 h	Reduced inflammation and cell apoptosis in rats

	IL-1Ra DNA	150 nm	65% over 15 days	NR
CS	BSA [93]	250 – 300 nm	45% over 7 days	NR
Silk fibroin	Cy7 (model drug) [102]	4 – 7 μm	3 – 8% over 7 days	Fluorescence half-life in rat joints of 43 h
	CXB and curcumin [106]	110 nm	4 – 30% over 56 h	NR
Poly(L-glutamin acid)-Poly(L-arginine)	IGF-1 [107]	100 – 850 nm	NR	System was detected in rat joints for 4 weeks; Reduced cartilage damage and enhanced aggrecan production
PLGA	TA [112, 113, 114]	35 – 55 μm	NR	TA detected in plasma of human patients after 12 weeks; Significant change in WOMAC compared to free drug; Reduced daily pain to week 12 compared to placebo but not to free drug
	Rhein [120, 121]	190 nm, 4 μm	45% over 24 h	NR
	NH_4HCO_3 and HA [125]	200 nm	70% over 10 days (pH 7.4); 80% over 2 days (pH 5)	IR-780-loaded particles detected in mouse joints for 35 days; Qualitatively appeared to slow OA progression
	OXC [126]	90 – 500 nm	50% over 2 – 9 days	NR

	P47phox siRNA [129]	130 nm	48 h	Reduced allodynia in OA rats
	p66shc [130]	184 nm	48 h	Reduced pain behavior, cartilage damage and inflammatory cytokine expression in rats
	AlexaFluor (model drug) [132]	170 – 200 nm	NR	Non-targeted, cationic, and peptide-targeted particles exhibited similar joint retention in healthy rat joints, but peptide-targeted particles were retained more in OA than healthy joints
	Rapamycin [133]	1 μm	48 h – 21 days	Cy7-labeled particles detectable for 30 days with half-life of 3.9 days in mouse joints
PLGA-PTE	CXB, TA [115]	37 – 55 μm	60 – 110 days	NR
PLGA-Eudragit RL	DiR [116]	170 nm	30% over 7 days	50% of DiR detected at 28 days in mice
	PRX [117]	220 nm	80% over 24 h	3.2-fold increase in joint tissue concentration of PRX compared to free drug (rats)
PLGA-gelatin	Fluvastatin [118]	25 μm	10 days	Reduced OARSI scores in rabbits
PLGA-lipid	MK-8722 [138]	25 nm	48 h	Reduced levels of pro-inflammatry cytokines,

				synovitis, and cartilage damage in mice
PDLLA	DiD [142]	300 nm, 3 μm, 10 μm	< 2% over 42 days	Particles observed in the joint for 6 weeks, with size-dependent clearance
	PH-797804 [143]	14 μm	20% over 3 months	Reduced inflammation and IL-1β expression in mice
	KGN [144]	14 μm	60% over 90 days	Reduced OARSI scores in mice
PCL	Doxycycline and CS [148]	12 – 75 μm	24 days	Improved radiographic scores and Mankin-Pitzer histology scores in rabbits
	Etoricoxib [150]	5 – 16 μm	90% over 20 days	Particles detectable over 4 weeks in rats
PEA	CXB [156]	10 – 100 μm	80 days but also stimuli-responsive	Particles detectable after 3 weeks but did not lead to reduced OA pathology in rats
	TA [160]	22 μm	50% over 60 days	Particles detectable for 70 days, decreased synovial inflammation but no clear effects on cartilage integrity in rats
	CXB [161]	640 – 1040 nm	30 – 80% over 60 days	Well tolerated in the joints of sheep
	GSK3787 [162]	580 nm	11% over 30 days	Particles detected in mouse joints over 7 days *ex vivo*

pNIPAM (various formulations)	KAFAK, YARA [166, 168-171]	100 – 400 nm	Variable from 24 h – 50% over 4 days	Particles penetrated through inflamed bovine cartilage explants and reduced IL-6 production
	HA [167]	130 – 240 nm	NR	Protected cartilage and reduced pro-inflammatory cytokines in mice
pNIPAM-HA	DCF [175]	200 μm	10 days	Reduced cartilage damage and lowered OARSI scores in rats
p(NIPAM-MPC)	DCF [173]	145 – 200 nm	88% over 72 h	NR
pMPC-silica	DCF [174]	260 nm	72 h	Reduced cartilage damage and OARSI scores in rats
PVA	Fluticasone propionate [176]	50 – 100 μm	NR	Drug detected in synovial fluid and cartilage of dogs for 60 days
pHEMA	IL-1Ra, BSA [179, 180]	300 – 900 nm	NR	30% of labeled BSA retained at 14 days in rat joints
PEG-PLA	FITC (model drug) [181]	256 nm	NR	Particles bound to cartilage tissue sections *ex vivo*
	Adenosine [183]	129 – 144 nm	NR	Reduced OARSI scores and cartilage loss in rats
PEG-PCL	TGFα [184]	26 nm	NR	Reduced cartilage damage, synovitis, pain,

				and subchondral bone thickening in mice
Polyurethane	KGN [182]	25 nm	20% over 15 days	Reduced cartilage damage and OARSI scores in rats
PAMAM dendrimer	KGN [189]	35 nm	NR	60% of dendrimer detected in rat joints after 3 days
	IGF-1	NR	NR	Reduced cartilage degradation, synovial inflammation, and osteophyte burden in rats

2. Biopolymer-based particles

Biopolymers are natural polymers including nucleic acids, polypeptides, and polysaccharides that are synthesized by living organisms. In particular, polypeptides [62] as well as polysaccharides including chitosan [63], HA [64], and alginate [65] have been extensively investigated for drug delivery and tissue engineering. These materials can be degraded enzymatically, and can have favorable biological properties, as they are found naturally within or mimic components of the native ECM within human tissues. However, challenges for natural materials include batch-to-batch reproducibility in their isolation and processing, as well as limitations in the extent to which one can tune their chemical and mechanical properties [66].

2.1 Chitosan

Chitosan is cationic polysaccharide that is obtained by deacetylation of chitin, a structural component of the exoskeletons of crustaceans. It is a random copolymer of β-(1-4)-linked *N*-acetyl-D-glucosamine and D-glucosamine (**Figure 2A**). It has been widely used in biomedical applications such as wound healing and also in drug delivery because of its biodegradability,

biocompatibility, and the presence of the amino groups, which allow for its functionalization [67-69].

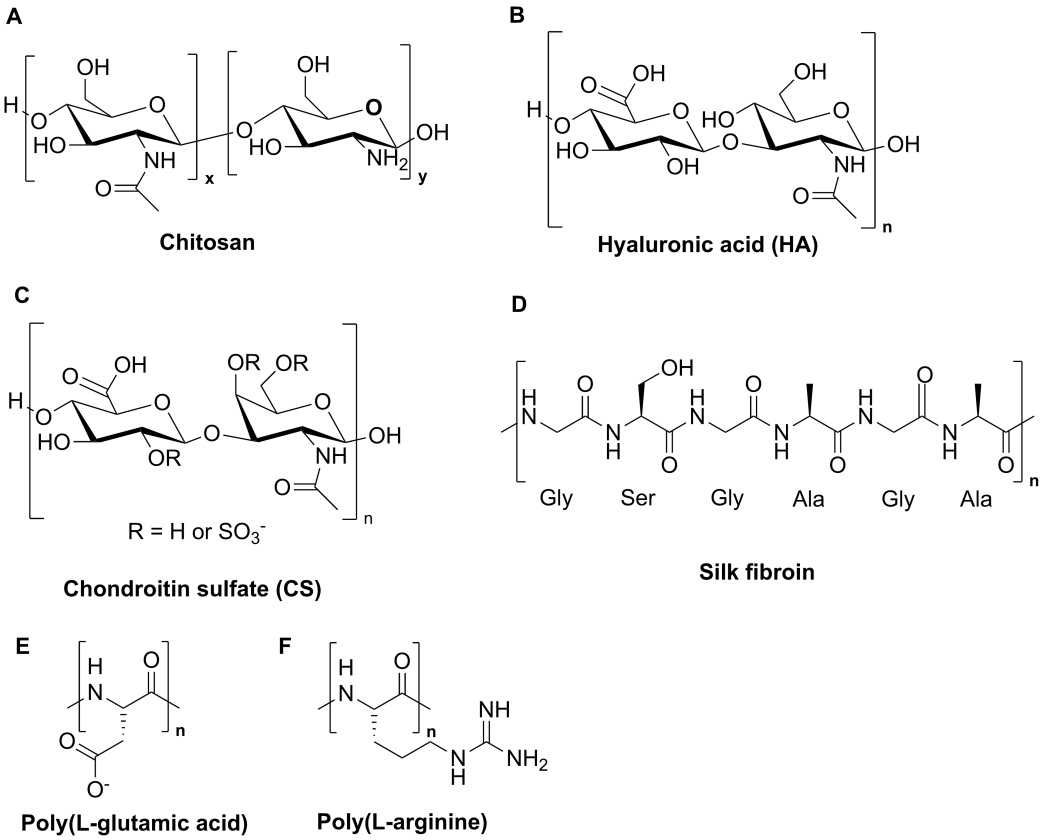

Figure 2. Chemical structures of biopolymers used in IA drug delivery systems: A) chitosan; B) HA; C) CS; D) the main primary structure of silk fibroin; E) poly(L-glutamic acid); F) poly(L-arginine).

Chitosan particles were prepared by Kamel and coworkers for the IA delivery of the NSAID lornoxicam with the goal of reducing its side effects [70]. The particles were prepared by ionic gelation with tripolyphosphate (TPP), a process involving the entropically and electrostatically-favorable self-assembly of polyanions with polycations (**Figure 3**). Lornoxicam was loaded during the particle preparation, leading to encapsulation efficiencies ranging from 14 – 60% and average particle diameters from 3.6 to 6.1 μm, depending on the conditions. Complete release of the drug was observed *in vitro* over 8 days. The anti-inflammatory effects of the particles were examined and compared to those of the free drug *in vivo* in a monoiodoacetate (MIA)-induced OA model in rats. Reduced inflammation and histopathological markers of OA

were observed for the drug-loaded particles, compared to the free drug and controls over the 21 day study, suggesting that slow release of the drug was beneficial. However, to achieve benefits over a longer time period, it may be necessary to further slow the release of the drug.

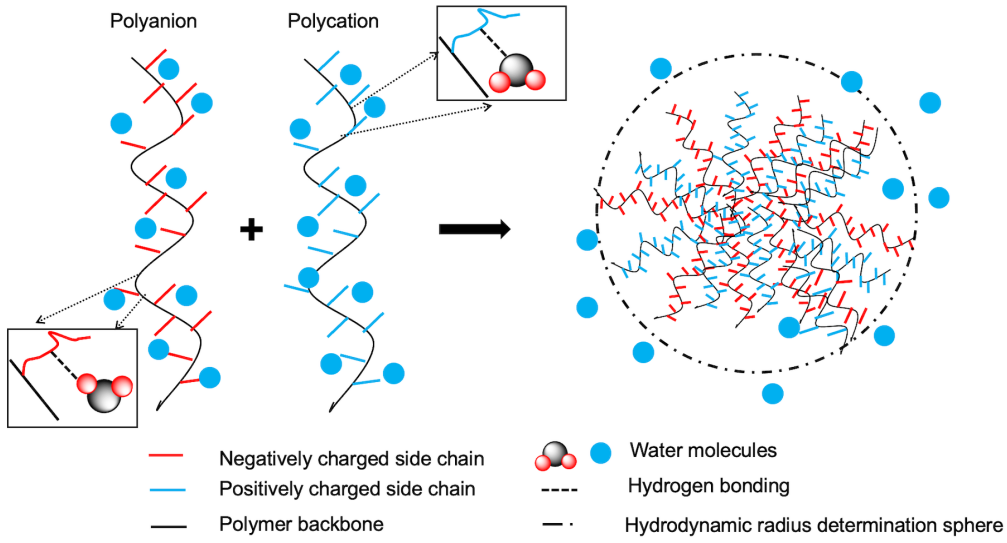

Figure 3. The process of complexation between polyanions and polycations to form a nanoparticle. The process is driven by the entropically favorable release of water.

Fan and coworkers encapsulated sinomenium into chitosan particles [71]. Sinomenium is a natural alkaloid that has been shown to modulate NF-κB signaling, down-regulate MMP-13 expression, and regulate autophagy, a protective mechanism in normal joints [72, 73]. The particles were prepared by a water-in-oil (w/o) emulsion process (**Figure 4A**), in which the drug was combined with chitosan in the aqueous phase, and then the chitosan was crosslinked using glutaraldehyde. They had an average diameter of about 100 μm and released all of their loaded sinomenium over 96 h *in vitro*. Next, the particles were loaded into photo-crosslinked gelatin methacrylate hydrogels, with no effect on the drug release rate. The sinomenium-loaded particle-containing gels were evaluated in a surgical mouse model of OA with once weekly injections. They reported that treatment with the drug-particle-gel system slowed the progression of OA and mitigated cartilage degradation at least partly by inducing autophagy. Unfortunately, details were not reported on how the authors performed photo-initiated crosslinking after injection of their materials into the joint, so it would be difficult to reproduce this work.

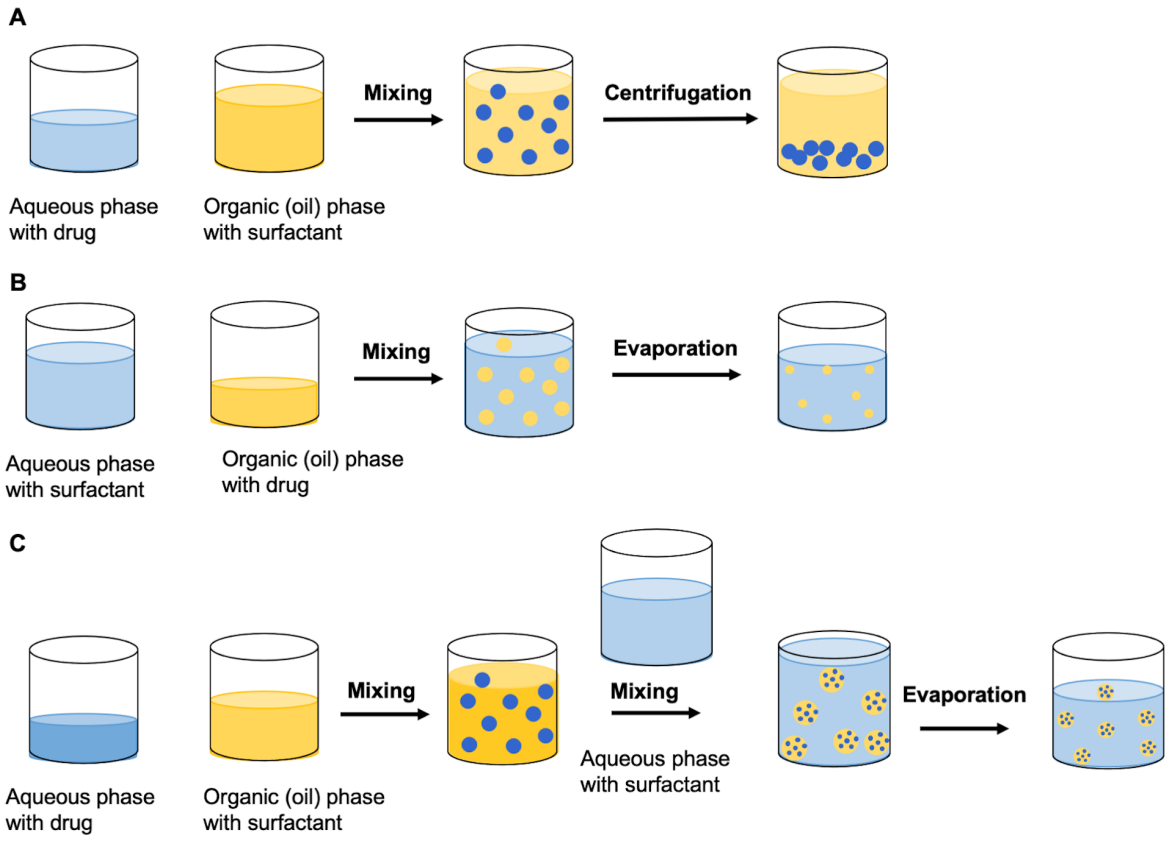

Figure 4. Schematics of the particle preparation procedure by A) water-in-oil (w/o) emulsion; B) oil-in-water (o/w) emulsion; C) double emulsion (water-in-oil-in-water, w/o/w).

Im and coworkers prepared and studied kartogenin (KGN)-functionalized chitosan particles [74]. KGN is an activator or the core binding factor β/runt-related transcription factor 1 (CBFβ/RUNX1) pathway, that can promote the chondrogenic differentiation of mesenchymal stem cells (MSCs) [75, 76]. First, KGN was coupled to chitosan using a carbodiimide-promoted amide bond formation. The conjugation efficiency was reported to be high (> 97%), though the extent of chitosan functionalization was not very clear in the paper. Our analysis of the presented spectral data suggests that about 1% of chitosan's amino group were coupled to KGN. Next, nanoparticles (150 nm) and microparticles (1.8 μm) were prepared from the modified chitosan by ionic gelation with TPP. *In vitro* release studies showed that 30 – 50% of KGN was released over 7 weeks, with the microparticles having higher release than the nanoparticles. Both particles induced higher expression of chondrogenic markers from human bone marrow MSCs. Retention of fluorescently-labeled particles in the joints of rats was observed for 24 days. In a surgically-

induced OA model, rats treated with the particles 6 and 9 weeks after surgery, and analyzed at 14 weeks exhibited less cartilage damage as indicated by lower Osteoarthritis Research Society International (OARSI) scores and less marked biochemical changes based on immunofluorescence for collagen type 2 and aggrecan. The results were similar for the two particle sizes. These results suggested that KGN may have led to regenerative effects in cartilage, though explicitly proving regeneration would require analysis at multiple end points.

In follow-up work, Im and coworkers further developed their delivery system by covalently crosslinking the KGN-chitosan conjugate with thermoresponsive poloxamer 407, a poly(ethylene oxide (PEO)-*block*-poly(propylene oxide) (PPO)-PEO triblock copolymer, containing two terminal carboxylic acids [77] (**Figure 5**). In addition, the anti-inflammatory drug diclofenac (DCF) was loaded into the hydrophobic PPO core of the resulting assemblies at low temperature. The diameter of the assemblies changed from 650 nm at 4 °C to 305 nm at 37 °C. The release of both drugs was faster at lower temperature presumably due to increased swelling and water access to the particle core. The release of non-conjugated DCF was faster than that of covalently conjugated KGN. *In vitro*, both chondrogenic differentiation and suppression of inflammation were enhanced by cold shock treatment. The particles were retained in rat joints for up to 14 days and they suppressed the progression of OA in rats relative to controls, with cold treatment leading to enhanced efficacy. Overall, the biological properties of KGN are interesting for potential OA treatment. However, in our own unpublished work, we found that KGN is highly susceptible to intramolecular cyclization under coupling conditions, which can make its conjugation chemistry challenging.

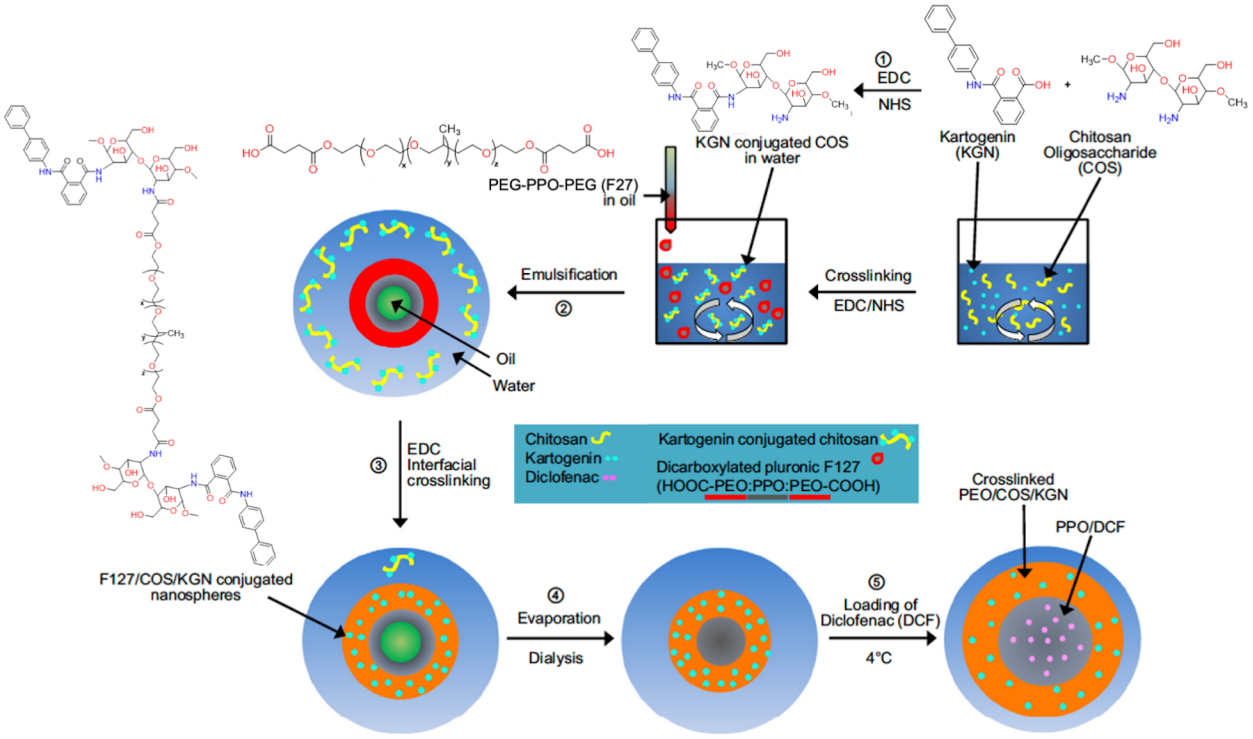

Figure 5. Schematic illustrating the process for preparing a thermoresponsive KGN delivery system: 1) synthesis of the KGN-chitosan conjugate using *N*-ethyl-*N*′-(3-dimethylaminopropyl)carbodiimide (EDC) and *N*-hydroxysuccinimde (NHS); 2) o/w emulsification of the PEO-PPO-PEO; 3) coupling of PEO-PPO-PEO with the chitosan-KGN conjugate using EDC; 4) evaporation and dialysis to remove reagents and the organic phase; 5) loading of DCF. Modified from reference [77] with permission from Elsevier.

Liu and co-workers investigated chitosan particles loaded with berberine chloride [78], an isoquinoline alkaloid shown to reduce chondrocyte apoptosis and promote cartilage matrix production [79]. The particles were prepared by ionic gelation using TPP, and berberine was loaded during the preparation. They had diameters ranging from about 50 to 400 nm based on dynamic light scattering (DLS) and scanning electron microscopy (SEM). About 70% of the loaded berberine was released *in vitro* over 7 days. *In vivo*, berberine was detected in the synovial fluid of treated rats for at least 96 h, whereas the injected free drug was no longer detected in synovial fluid after 48 h. In addition, in a surgical rat model of OA, the particles led to enhanced anti-apoptosis activity and cartilage protective effects compared to the free drug and controls, suggesting their potential for OA treatment.

Clodronate-loaded chitosan nanoparticles were prepared and studied by Caviglioli and co-workers [80]. Clodronate is an anti-osteoporotic drug that acts by inhibiting metabolism in osteoclast mitochondria. However, it has also be found to exhibit anti-inflammatory and anti-arthritic activity. These effects have been proposed to arise from its ability to reduce articular inflammatory lesions by inhibiting the synthesis and release of pro-inflammatory mediators such as cytokines and nitric oxide by macrophages [81]. However, it can cause gastrointestinal disorders and nephrocalcinosis, particular when given orally [82]. The authors prepared the particles by ionic gelation between chitosan and clodronate, which contains two anionic phosphonates. The chitosan amino groups were then crosslinked with glutaraldehyde, providing cationic particles with an average diameter of 146 nm and a drug loading of 31% w/w. Over 48 h *in vitro*, 90% of the clodronate was released from the particles. The clodronate-loaded particles were more effective than the free drug at reducing the pro-inflammatory response of THP1 macrophages to lipopolysaccharide. To slow the drug release and increase their retention times in the joint, the particles were encapsulated into thermoresponsive poloxamer gels, which existed as viscous liquids at room temperature and below, but gelled at about 30 °C. The gel encapsulation slowed the *in vitro* drug release during the first 24 h, resulting in close to zero-order kinetics. These results suggest that the gel was able to provide a desirable steady release of drug during this time period, but after 48 h, about 80% of the drug was released, which was quite similar to the percentage released by the particles alone. Overall, the rapid release of clodronate from these delivery systems raises questions regarding the benefit of of the delivery system compared to administration of the free drug.

Qiu and coworkers exploited chitosan's cationic charge to bind with anionic DNA encoding the gene for cytokine response modifier A (CrmA) [83], a natural inhibitor for IL-1β converting enzymes, which subsequently reduces IL-1β induced inflammation associated with chondrocytes in OA [84, 85]. The particles, designed to carry the CrmA gene into cells, were prepared by ionic complexation between the DNA and chitosan. They had diameters of about 50 nm based on SEM. DNA release from the complexes was evaluated at pH 2 and pH 7. At pH 7, about 60% of the DNA was released over 7 days, whereas about 35% was released at pH 2 over the same time period. It is not clear why pH 2 was selected, as this pH value is not relevant to the intracellular environment or joint tissues. After confirming the successful transfection of primary

rabbit chondrocytes with CrmA, the particles were evaluated in a surgical rabbit model of OA. Weekly doses of the particles for 4 weeks resulted in reduced cartilage degradation, a reduction in mRNA levels of MMPs and IL-1β, and reduced chondrocyte apoptosis compared to controls. Overall, these results suggest the therapeutic potential for the chitosan-CrmA DNA particles.

2.2 HA

HA is an anionic glycosaminoglycan composed of repeating β-(1-4)-D-glucuronic acid and β-(1-4)-*N*-acetyl-D-glucosamine units (**Figure 2B**). In the synovial fluid of healthy joints, HA has an average molar mass of 3 – 4 million g/mol and has an important role in the fluid's lubrication and viscoelasticity [86]. HA's molar mass and concentration decrease as OA progresses, so it has commonly been used in the treatment of OA. Despite the questionable clinical efficacy of HA treatments alone, its routine use in joints has made HA a popular choice as a component of OA delivery vehicles.

Korkusuz and co-workers prepared nanoparticles based on HA and glucosamine [87]. Oral glucosamine is taken as a supplement by some OA patients, but can be problematic for diabetic patients [88] and only a tiny fraction of the dose ever reaches the joint [89], motivating the authors to deliver it directly to the joint with HA. To prepare the particles, 5-β-cholanic acid was conjugated to HA as a hydrophobe, and then amino-terminated PEG was also conjugated to the HA. The resulting copolymers were assembled into core-shell particles with PEG surfaces, and finally GA was physically immobilized. The authors proposed that the glucosamine was preferentially located within the hydrophobic PEG domains, but since it is cationic at neutral pH it was presumably at least partially complexed with the remaining carboxylic acid groups on the HA. Using SEM and DLS, the average particle diameters were found to be 175 nm and 187 nm respectively. *In vitro* release studies revealed that 20% of the glucosamine was released over 21 days, which is surprisingly slow for a hydrophilic payload in the absence of covalent conjugation. *In vitro*, released glucosamine reduced the proliferation of chondrosarcoma cells. However, there were no changes in OA or ECM markers of healthy or OA chondrocytes at 7 days, suggesting that the molecules were not active at the cellular level.

CXB-loaded HA nanocapsules were examined by El-Gogary and coworkers for IA delivery [90]. The particles were prepared by a nanoprecipitation approach involving the

addition of an ethanol/acetone solution of CXB, olive oil, and cetyltrimethylammonium bromide to an aqueous solution of HA and either polysorbate 80 or poloxamer P407 as a surfactant, followed by evaporation of the organic solvent. The average particle diameters ranged from 250 – 450 nm. *In vitro*, the particles released all of their CXB from the oil core over 7 days. In a rat MIA model of OA, the 250 nm particles reduced swelling, cartilage damage, and NF-kB expression compared to the free drug and non-treated controls.

HA has also been combined with chitosan for particle preparation. For example, Tao and co-workers encapsulated curcuminoid during ionic gelation of the polymers [91]. Curcuminoids have been suggested to inhibit the apoptosis of chondrocytes as well as inflammatory signaling in OA [92], but exhibit very low aqueous solubility and poor bioavailability when administered orally. The resulting particles had an average diameter of 165 nm based on TEM and a high drug loading capacity of 38%. During a 72 h *in vitro* release study, the particles released of 74% of the curcuminoid compared to 84% for the non-encapsulated drug. The fact that the delivery system only slowed the release to a small extent suggests that the release rate was likely limited by the low solubility of curcuminoid in the release medium. Consequently, it appears that the delivery system is not able to provide sustained drug release. In a rat surgical model of OA, IA injection of the drug-loaded particles attenuated inflammation and cell apoptosis compared to controls, and this change was proposed to occur through repression of the NF-kB signaling pathway. The particles also promoted collagen type 2 expression and decreased MMP-1 and MMP-13 expression, suggesting their potential for OA therapy.

Zhou and co-workers prepared ionically complexed HA-chitosan nanoparticles encapsulating plasmid DNA for IL-1Ra, a competitive inhibitor for IL-1β [93]. The goal was to transfect synoviocytes to overexpress IL-1Ra, thereby attenuating IL-1β-induced inflammation [94]. A chitosan:HA ratio of 4:1 led to particles with average diameters of about 150 nm based on DLS and SEM. An *in vitro* release study showed 65% release of the DNA after 15 days. The delivery system increased the expression of IL-1Ra in primary synoviocytes and reduced the expression of cyclooxygenase-2, inducible nitric oxide synthase, MMP-3, and MMP-13 in IL-1β-induced synoviocytes. However, no *in vivo* experiments were performed. In follow-up work, the team used the same delivery system for CrmA, achieving similar *in vitro* results [95].

2.3 CS

CS is a sulfated glycosaminoglycan composed of alternating glucuronic acid and *N*-acetylgalactosamine moieties (**Figure 2C**). It is an important component of aggrecan proteoglycans, which form a dense network with collagen fibrils in cartilage [96]. Because of its role in joint tissues, it has been used as a dietary supplement, though well controlled trials have failed to demonstrate significant clinical benefits relative to placebo in providing relief for knee OA [97]. Nevertheless, as a polymer intrinsically present in joints, CS has been investigated for IA drug delivery, particularly as a polyanion for the formation of ionic complexes with chitosan.

Young and coworkers prepared particles composed of CS and N-[(2-hydroxy-3-trimethylammonium)-propyl]chitosan chloride (HTCC) by ionic gelation [98]. By varying the CS:HTCC ratio, anionically or cationically charged complexes were obtained. Fluorescein-labeled bovine serum albumin (BSA), as a model protein drug, was loaded in the particles during their preparation. The resulting particles had average diameters of 250 – 300 nm depending on the BSA concentration during loading. In buffer at pH 7.4, about 45% of the BSA was released from the complexes over 7 days. The particles exhibited low cytotoxicity *in vitro* but further studies will be needed to determine the potential of this system for applications in OA drug delivery.

Rhamdhani formulated particles from CS with kappa carrageenan and chitosan [99]. Depending on the ratios of the polymers, the average diameters of the particles ranged from 580 – 920 nm, and the particle charge could also be tuned. However, no biological studies were performed on these particles. Overall, as CS would be expected to be well tolerated in the joint, further studies are warranted on CS-based IA drug delivery vehicles.

2.4 Polypeptides

Nature uses polymers of amino acids to achieve a diverse array of functions from catalysis to structural support, with the specific structures and functions defined by the sequence of amino acids. Polypeptides have also been garnering interest in drug delivery applications due to their highly tunable properties [100, 101]. Several polypeptides have been investigated for the IA delivery of potential OA therapeutics.

Setton and coworkers investigated silk fibroin (**Figure 2D**) microparticles for sustained release of molecules in joints [102]. Silk fibroin is a natural protein material obtained by de-

gumming native silk fibers. It is highly hydrophobic, forming β-sheet structures, and its high crystallinity imparts slow degradation *in vivo* [103, 104]. It is also non-immunogenic [105]. In their study, the authors conjugated the fluorescent dye Cyanine 7 (Cy7) as a model drug molecule to the primary amino group on the protein, and then prepared particles from a mixture of the conjugate and unmodified protein by an emulsion method. The mean diameters of the particles ranged from 4 – 7 μm, depending on the ratio of the Cy7-labeled to unlabeled proteins. Under proteolytic conditions *in vitro*, the particles released 3 – 8% of the Cy7 over 7 days, showing their potential for sustained release relative to the polysaccharide-based particles described above. IA retention in rat joints was measured by live-animal fluorescence imaging. The half-life of fluorescence decay was 43 h for the Cy7-conjugated particles compared to 13 h for free Cy7, and the particles were more localized in the joint capsule than the free dye, suggesting the potential of the silk fibroin particles for sustained IA drug delivery (**Figure 6**).

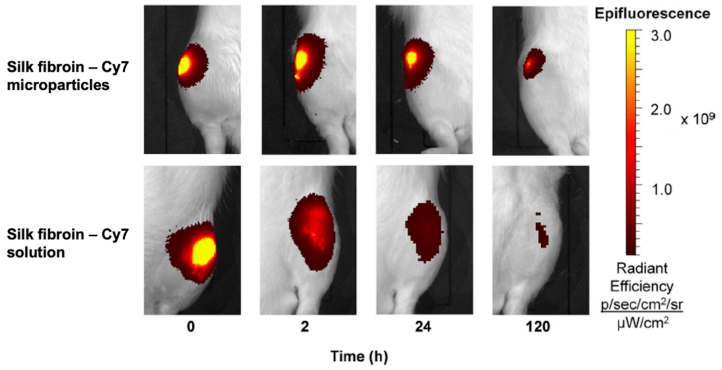

Figure 6. *In vivo* epifluorescence imaging of Cy7-labeled silk fibroin particles after IA injection in rats compared to a solution containing non-encapsulated Cy7. The particles resulted in a more persistent and focused fluorescence over 120 h. Reproduced from reference [102] with permission from Elsevier.

Perteghella and coworkers investigated silk fibroin particles for the CXB and curcumin delivery [106]. The particles were prepared by a desolvation method involving the addition of silk fibroin solution to acetone containing the drug. The resulting particles had mean diameters of about 110 nm and contained either 5 or 11 % w/w of CXB or 1.5 % w/w curcumin. *In vitro*, 14 – 30% of the drug was released over 56 h, showing the potential of the particles for sustained release. The faster release of drug from these particles compared with those studied by Setton

can likely be attributed to the higher surface:volume ratio of these smaller particles, as well as the fact that in this case the drug was not covalently conjugated. The particles exhibited reactive oxygen species scavenging ability, high hemocompatibility, and low cytotoxicity to human articular chondrocytes compared to the free drugs. They also provided anti-inflammatory activity in IL-1β-stimulated chondrocytes.

Ionic complexes of poly(L-glutamic acid) (**Figure 2E**), poly(L-arginine) (**Figure 2F**), and IGF-1 were investigated by Hammond and coworkers with the aim of achieving delivery to chondrocytes in cartilage [107]. IGF-1 is a pro-anabolic growth factor that has been shown to stimulate chondrocytes to produce ECM [108]. Various molar ratios of the polymers were assembled, leading to particles with average diameters ranging from 100 – 850 nm based on DLS. The diameters were much smaller based on cryo-TEM (17 nm), suggesting that DLS was detecting aggregates of individual particles. All of the prepared particles were cationic, as the aim was to achieve penetration into cartilage, which is anionic. Both the complex and free IGF-1 increased sulfated glycosaminoglycan synthesis in *ex vivo* cartilage disks from bovine joints. Both the complex and free IGF-1 exhibited similar penetration into the cartilage disks. The efficacy of the complexes was then compared to free IGF-1 in a surgical rat model of OA and the complexes and free drug were tracked using a near-infrared fluorescence reporter. The free IGF-1 was cleared within a few days of administration, while the complexes were detectable in the joint for about 4 weeks. Only the complex was able to suppress IL-1β expression in the joint in a sustained manner over the course of the 30 day study. The complex also led to less cartilage damage and enhanced aggrecan production by chondrocytes in the deep zones of the cartilage. Overall, this study was critical in demonstrating the potential for polymer complexes to enhance both the joint residence time and cartilage penetration of a potential OA therapeutic.

3. Synthetic polymers

Synthetic polymers are non-natural macromolecules whose backbone is synthesized from monomers, which can come from either petroleum or renewable natural resources. In comparison to biopolymers, they have the advantage of having highly customizable structures, as a wide range of monomers with different functional groups can be incorporated into synthetic polymers. This customizability allows their mechanical properties, degradation rate, and biological properties to be tuned. In addition, compared to the process of isolating and purifying materials

from natural sources, synthetic processes are often highly reproducible, leading to polymers with reproducible properties on a batch-to-batch basis. On the other hand, while biopolymers such as HA or CS are found naturally in human tissues and can have favorable biological properties for some applications, synthetic polymers can lack these biological cues. In addition, they must be carefully designed to avoid the generation of toxic degradation products.

3.1 Poly(lactic-*co*-glycolic acid) (PLGA)

PLGA, a copolymer of lactic acid and glycolic acid (**Figure 7A**), has been the most widely investigated polymer for the preparation of particles for IA delivery. It has been extensively studied in the biomedical field for the controlled release of numerous therapeutics and is used clinically in a number of drug formulations for the treatment of cancer, growth deficiencies, acromegaly, and other conditions [109, 110]. Its degradation leads to lactic acid and glycolic acid, which are easily metabolized to carbon dioxide and water by the body, and its degradation rate and drug release properties can be tuned to some extent by adjusting the polymer molar mass, monomer ratio, and the content of loaded drug [111].

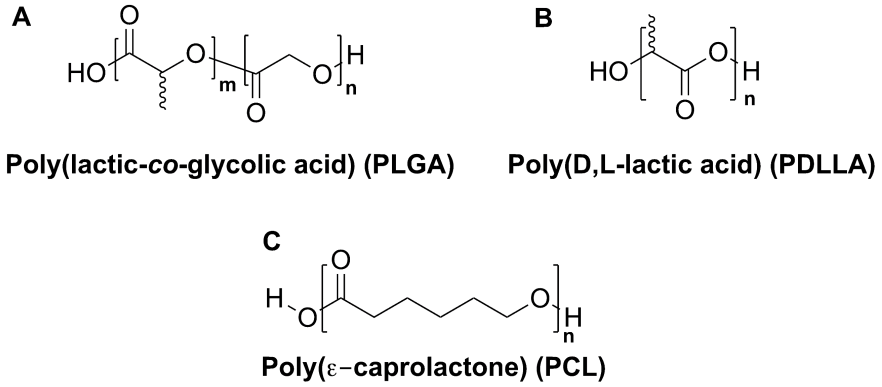

Figure 7. Chemical structures of polyesters commonly used for drug delivery: A) PLGA; B) PDLLA; C) PCL.

The most noteworthy example of a PLGA particle system for IA delivery is FX006, which was approved by the United States Food and Drug Administration in 2017, as the only extended-release IA therapy for OA-related knee pain. FX006 contains 25% w/w of triamcinolone acetonide (TA) crystals (< 5 μm diameter) encapsulated in PLGA composed of 75:25 lactic acid:glycolic acid (**Figure 8**) [112]. The resulting particles have a mean diameter of 42 μm and size range of 35 – 55 μm. *In vitro*, the particles do not exhibit a burst release, but

rather a continuous slow release of drug. In a rat model of synovitis, FX006 reduced pain over a longer duration than a TA crystalline suspension (TAcs), and FX006 significantly improved histological joint scores, whereas TAcs did not [113]. In a Phase 2, open-label study involving 81 patients, the pharmacokinetics of FX006 and TAcs were compared [114]. Following IA injection of FX006, synovial fluid concentrations were 230000 pg/mL after 1 week, 3600 pg/mL at week 6, and 290 at week 12, whereas after IA injection of TAcs only two of eight patients had quantifiable TA after 6 weeks (7.7 pg/mL). Plasma levels of TA after FX006 administration reached a peak of 840 pg/mL over 24 h, and then declined gradually to < 110 pg/mL after 10-20 weeks. After IA injection of TAcs, plasma levels peaked at 4 h (9600 pg/mL) and dropped to 150 pg/mL at week 6. These results showed that the delivery system was capable of prolonging the joint resident time of TA, while reducing the systemic exposure to the drug, thereby potentially mitigating steroid side effects. In a double-blinded, multicenter, 24-week Phase 3 study, 484 patients received FX006, saline placebo, or TAcs [112]. The change in average daily pain from baseline to week 12 for FX006 compared to the placebo was the primary end point and was met in the study. A 50% improvement in average daily pain intensity was observed, compared to the placebo; however, despite the greatly increased retention of TA in the joint after administration of TAcs observed in the pharmacokinetic studies, the reduction in pain compared to TAcs was not significant for FX006. In contrast, 12 week changes in the Western Ontario and McMaster Universities Osteoarthritis Index (WOMAC) and Knee Injury and Osteoarthritis Outcome Score Quality of Life were significant for FX006 compared to both TAcs and the placebo. Average daily pain increased for patients undergoing both steroid treatments from 6 – 8 weeks onward. Overall, these results highlight the limitations of steroid treatment, in terms of their lack of ability to provide long-term disease-modifying effects for OA treatment.

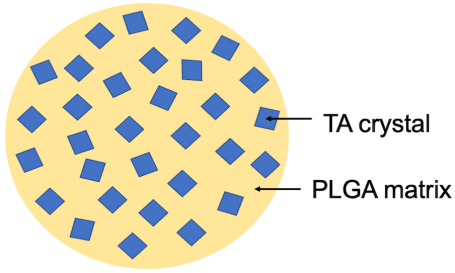

Figure 8. Representation of FX006 consisting of TA crystals (blue) in a PLGA matrix (yellow) (not to scale).

Creemers and coworkers prepared and studied particles composed of PLGA containing polythioester linkages (PLGA-PTE, **Figure 9**) and loaded with either CXB or TA [115]. PLGA:PTE ratios of 50:50 and 75:25 were compared. The microspheres were prepared by a double emulsion (water-in-oil-in-water, w/o/w) method (**Figure 4C**), resulting in mean diameters of 40 - 55 μm for CXB-loaded microspheres, and about 37 μm for the TA-loaded microspheres based on laser diffraction. The loading content of CXB was 7 and 8% w/w and that of TA was 11 and 9% w/w for PLGA-PTE 50:50 and PLGA-PTE 75:25 respectively. *In vitro*, complete release of CXB occurred over about 60 – 110 days, with the 50:50 system releasing CXB more rapidly. Release was fastest during the first 14 days, with about 50% of the drug released. The TA-loaded microspheres released the drug more rapidly, with 50% released during the first week and more than 90% released by day 28. As noted by the authors, the presence of surfactant in the *in vitro* release medium may have influenced the release kinetics by altering the particle stability and structure. Therefore, the bioactivity of released drug was evaluated in an *in vitro* assay over 21 days. Prostaglandin E_2 (PGE_2) production from human chondrocytes stimulated by TNFα was measured to evaluate inflammation. CXB-loaded particles reduced PGE_2 production to 0 – 7% of the control values at a drug equivalent dose of 1 nmol for 21 days. At the same dose of drug, the TA-loaded particles suppressed PGE_2 production to 0 – 12% of controls until 15 days, but less effectively after that, perhaps due to the more rapid release of TA and thus its depletion in the particles. After co-incubation with the cells for 21 days, the microscopy images of the particles showed that substantial erosion of the particles had occurred, which was consistent with the observed release kinetics. Further studies would be needed to evaluate the effects of the PLGA-PTE particles in joints in suppressing inflammation associated with OA.

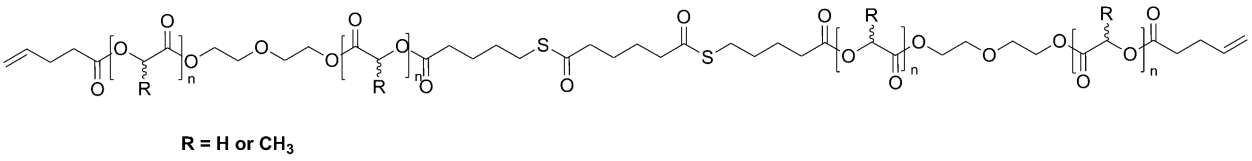

Figure 9. Chemical structure of PLGA-PTE.

Choi, Kang, and coworkers prepared particles from PLGA and Eudragit RL, a cationic polymer prepared from ethyl acrylate, methyl methacrylate, and a methacrylic ester with a

quaternary ammonium group [116]. These cationic particles were designed to interact electrostatically with anionic HA in synovial fluid, increasing their retention time in the joint. The particles were prepared by an oil-in-water (o/w) emulsion method (**Figure 4B**), with a PLGA/Eudragit RL ratio weight ratio of 70:30, and 0.1% w/w of poly(vinyl alcohol) (PVA) in the external phase. The average diameter was 170 nm, and the zeta potential of the particles was 21 mV based on DLS. In initial work, a fluorescent probe, 1,1′-dioctadecyl-3,3,3′,3′ tetramethylindotricarbocyanine iodide (DiR), was loaded into the particles. Upon mixing with HA, micrometer-sized filamentous aggregates were observed by hyperspectral imaging. *In vitro*, about 30% of DiR was released over 7 days, but then no further release occurred over the next 3 weeks, suggesting that the dye was trapped in the aggregates and that the initial rapid release may have corresponded to surface-bound dye. *In vivo* florescence images of mice injected with DiR-loaded particle suspensions demonstrated that 50% of the DiR remained detectable after 28 days, whereas for mice injected with same amount of free DiR, the signal of the probe in mice dramatically dropped to ~ 30% after 3 days. In a follow-up study, the particles were loaded with piroxicam (PRX), a potent NSAID [117]. The resulting drug-loaded particles had an average diameter of 220 nm, zeta potential of 12 mV, and contained 4% w/w of PRX. These particles also formed micrometer-sized aggregates with HA. Interestingly, these particles released PRX much more rapidly than DiR, with 80% of the drug release *in vitro* over 24 h. After IA injection into rats, the time to reach peak plasma concentration (T_{max}), was 0.8 h for free PTX, and 3.8 h for the PRX-loaded particles. The drug concentration in joint tissue was 3.2-fold higher for PTX-loaded particles compared to the free drug at 24 h. Overall, while this work suggests the potential for cationic nanoparticles to be retained in joints for weeks, the release of drug from the particles themselves should likely be slowed further to provide a more sustained supply of drug to joint tissues after injection.

Okazaki and coworkers studied microspheres composed of PLGA and gelatin as a delivery system for fluvastatin [118], a statin with anti-inflammatory effects, but severe side effects when administered systemically [119]. The particles were prepared by a double emulsion method (w/o/w) with gelatin and fluvastatin incorporated into the internal aqueous phase. The particles were about 25 μm in diameter and contained 3% w/w of drug. *In vitro*, the particles rapidly released 70% of their drug over 3 days, and the remainder over the next 10 days. Chondroprotective effects of fluvastatin were shown on primary human chondrocytes, as

indicated by promotion of collagen type 2 and aggrecan gene expression and inhibition of MMP13 gene expression. In a rabbit surgical model of OA, 5 weeks after IA injection, histological analysis showed lower OARSI scores for the animals treated with drug-loaded particles, compared to the control groups, showing the potential of this drug delivery system for further exploration.

Rhein-loaded PLGA particles have been investigated by Gómez-Gaete and coworkers [120, 121]. Rhein is an active metabolite of diacerein, an anthraquinone derivate with inhibitory effects on IL-1β but with low oral bioavailability and side effects associated with its systemic administration [122, 123]. The particles were prepared by an o/w emulsion method using PVA as a surfactant, resulting in a mean diameter of 4 μm and a drug loading of about 1% w/w [120]. *In vitro*, the particles released 45% of the drug during the first 24 h, suggesting that a large fraction of drug was adsorbed to the particle surface. The remainder of the drug was released more slowly over 30 days, even though intact particles could still be observed by SEM at this time point. The rhein-loaded particles inhibited the production of reactive oxygen species (ROS) and IL-1β in lipopolysaccharide (LPS)-stimulated THP-1 macrophages, but they did not inhibit the production of TNFα. In a subsequent study, the authors investigated different particle preparation methods including single o/w emulsion, double emulsion, and nanoprecipitation to prepare smaller rhein-loaded PLGA particles [121]. The single emulsion method led to the highest drug encapsulation efficiency (38%), providing particles with a mean diameter of 190 nm based on DLS. Unfortunately, rhein was released very rapid *in vitro*, with 50% released in 5 min and complete release within 60 min. As for the larger rhein-loaded particles, the nanoparticles suppressed IL-1β production in LPS-stimulated THP-1 macrophages, and at high concentration (5.0 μM) suppressed ROS production. However, to achieve benefits beyond those of the free drug *in vivo*, it will probably be important to slow the release of rhein from the delivery system.

Cruz and workers developed a pH-sensitive PLGA particle system to take advantage of a proposed decrease in pH in regions of the synovial cavity [124] to release HA in the joint in a controlled manner [125] (**Figure 10**). Using a double emulsion method (w/o/w), ammonium bicarbonate (NH_4HCO_3) and HA were incorporated into the particle cores, while PLGA formed the particle shell. The authors hypothesized that at acidic pH, NH_4HCO_3 inside NPs would react with H^+, producing CO_2, NH_4 and H_2O, subsequently causing the particle shell to rupture and

release HA. As probes, fluorescein isothiocyanate (FITC) or IR-780 were encapsulated. Based on DLS, the average diameter of the particles was about 200 nm. *In vitro* at pH 7.4, after an initial burst release of about 40% of HA, it was released more slowly, reaching about 70% release after 10 days. At pH 5.0, the release was more rapid, reaching 80% after 2 days. IR-780 did not undergo a burst release at pH 7.4, reaching 80% release over 30 days, whereas at pH 5.0 more than 90% was released within 2 days. The particles were well tolerated by and taken up by C28/I2 chondrocytes. After IA injection into mice with surgically-induced OA, the IR-780-loaded particles were detected by *in vivo* imaging over 35 days. The fluorescence signal from the joint decreased gradually but was still detectable at the last time point, suggesting a slow release and clearance of the dye, whereas the signal from injected free dye had completely disappeared. Treatment with the particles qualitatively appeared to reduce OA development, but small sample sizes prohibited quantitative comparisons between the groups, so the therapeutic potential of this HA delivery system remains unclear.

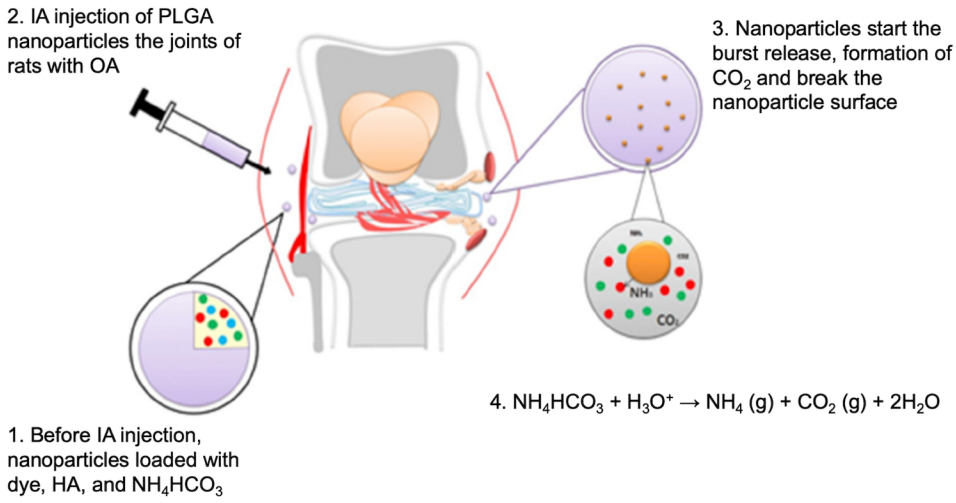

Figure 10. Schematic of pH-sensitive particles where encapsulation of NH_4HCO_3 leads to the generation of CO_2, rupturing the particles and releasing HA. Reproduced from reference [125] with permission from Elsevier.

Alarçin and coworkers prepared PLGA particles loaded with the anti-inflammatory drug oxaceprol (OXC) [126]. OXC is *N*-acetyl-L-hydroxyproline, which inhibits the inflammatory cascade by preventing granulocyte and leukocyte infiltration into joints and decreases the adherence of leukocytes to the blood vessel endothelium [127, 128]. The particles were prepared

by a double emulsion method, using PVA as the surfactant, resulting in particles with average diameters ranging from 90 to 500 nm based on DLS, depending on the drug loading (9 – 56% w/w). *In vitro*, 50% of the cargo was released over 2, 4, and 9 days for particles containing 56, 16, and 9% w/w respectively, and then the release rate slowed, with about 90, 80, and 60% of OXC released respectively after 30 days. *In vitro* cytotoxicity tests showed that OXC-loaded PLGA particles were well tolerated by human lymphoblastoid cells. Further work will be needed to determine whether they can successfully suppress inflammation associated with OA.

siRNA has also been incorporated into PLGA particles with the goal of reducing ROS in OA joint.[129, 130] Kim and coworkers investigated p47phox siRNA [129], as p47phox is an NADPH oxidase subunit that is believed to be involved in ROS production in the pathogenesis of OA [131]. The authors first conducted immunohistochemistry studies, showing that p47phox was highly expressed in human OA tissues collected from patients and in rat knees with MIA-induced OA. They then encapsulated p47phox siRNA into PLGA particles using a double emulsion method. The particles had an average diameter of about 130 nm based on DLS and SEM. *In vitro*, the particles released about 50% of the siRNA over 24 h and 95% over 48 h. Particles containing a fluorescent protein (mCherry) were observed in articular cartilage 3 days after injection into rat knees. The particles were then evaluated in a MIA-induced rat model of OA. The von Frey filament test indicated that p47phox siRNA-loaded particles alleviated mechanical allodynia in OA rats for up to 14 days after injection compared to controls. In addition, they led to reduced cartilage loss and reduced ROS production in cartilage.

In related work, similar particles were used by Kim and coworkers to deliver siRNA to another ROS production-related protein p66shc.[130] Elevated expression of this protein was also demonstrated through immunohistochemistry on tissues from OA patients and MIA-induced OA rats. Injection of these particles into rats with MIA-induced OA led to reduced pain behavior and cartilage damage, as well as reduced expression of inflammatory cytokines including TNFα, IL-1β, and cyclooxygenase 2 (COX2). Overall, these studies support the potential for siRNA treatments for OA, but to enhance their long-term efficacy, it may be desirable to extend the release of siRNA from these systems beyond 48 h.

Sharma and coworkers explored the effect of cartilage-targeting groups on the distribution of particles in healthy and OA joints [132]. The authors used an o/w emulsion method to prepare PLGA particles using PVA as a surfactant. Poly(allylamine hydrochloride) (PAA) was incorporated to make the surfaces of the particles cationic, facilitating their electrostatic interaction with the anionic cartilage matrix. In addition, the collagen type 2 binding peptide WYRGRLK was conjugated to the PAA surface using carbodiimide chemistry to provide particles with active targeting potential. All three particles had similar average diameters of 170 – 200 nm based on DLS. Despite their cationic charges, the PAA-coated particles exhibited low cytotoxicity to primary bovine chondrocytes and synoviocytes, as well as bovine cartilage explants. The uptake and retention of the three different particles, labeled with AlexaFluor, was first measured *ex vivo* in healthy cartilage and collagenase-treated cartilage as an OA mimic. In healthy tissue, the peptide-targeted particles exhibited 43% greater uptake than the non-targeted cationic and neutral particles. However, in the diseased tissue model, uptake of the non-targeted cationic particles reached a similar enhancement to the targeted particles. The peptide-targeted nanoparticles exhibited enhanced retention in both *ex vivo* models. The joint biodistribution of the particles was also evaluated in healthy rat knees and in rats with collagenase-induced OA. Within the healthy and OA groups, there were no differences in overall joint retention for the three types of particles. All of the particles, including the targeted one, were located primarily in the extensor mechanism. In OA joints, the peptide-targeted particles associated more with the femoral cartilage (21%) than they did in healthy joints (12%), suggesting their potential for effective delivery to diseased cartilage. These results highlight the importance of particle design and the challenges in achieving effective delivery into cartilage.

Rapamycin was encapsulated into PLGA particles by Agarwal and coworkers [133]. In animal models, rapamycin has been shown to slow OA progression, with its mechanism of action presumed to involve the induction of autophagy, an important process involved in tissue homeostasis [134]. In addition, it is also proposed to prevent chondrocyte senescence, which may be involved in promoting both age and trauma-induced OA [135, 136]. However, rapamycin exhibits side effects and toxicity at the high doses needed to achieve sufficient joint concentrations via systemic delivery [137]. Therefore, rapamycin was encapsulated into PLGA particles for IA delivery. The particles were prepared by an o/w emulsion method using PVA as a surfactant, resulting in a diameter of about 1 μm. The time required for complete release of

rapamycin ranged from 48 h to 21 days, depending on the PLGA composition, with higher molar mass resulting in slower release and a higher lactide:glycolide ratio also providing slower release. *In vitro* studies in immortalized human chondrocytes (C28/I2) showed that the particles induced autophagy and prevented senescence under genotoxic and oxidative stresses, and helped sustain glycosaminoglycan production. *In vivo* studies showed that Cy7 delivered via the particles into mouse joints resulted in a half-life of 3.9 days, compared to 1 day for the free dye and the particles could be detected for 30 days. While further studies will be needed to assess the potential of the rapamycin particles to prevent OA progression, this study affirms the potential of both the drug and the delivery system.

Gao, Zhang, and coworkers developed a lipid-PLGA delivery system designed to target cartilage [138]. The particles consisted of a PLGA core coated in PEG-modified lipid, with a conjugated collagen binding peptide WYRGRLC. The particles were 25 nm based on DLS, with the small size proposed to be important to enable cartilage penetration. DiD-labeled peptide-targeted particles exhibited about 2-fold higher penetration into the femoral heads of mice *ex vivo* than non-targeted particles. About 42% of DiD-labeled peptide-targeted particles were detected in mouse joints after 48 h compared to only 18% of non-targeted particles. MK-8722, an activator of 5'-adenosine monophosphate activated protein kinase, which is known to regulate chondrocyte metabolism [139], was then loaded into the PLGA core. The drug was released over about 48 h *in vitro*. In a mouse model of collagenase-induced OA, the drug-loaded particles reduced levels of pro-inflammatory cytokines such as TNFα, IL-1β, and nitric oxide synthase 2. In addition, the treated mice exhibited reduced synovitis and reduced cartilage damage based on histological analysis, compared to control mice. Overall, this delivery system is attractive as the phospholipid surface affords biomimetic properties, and the particle diameter is small enough to enable penetration into cartilage. However, for some therapeutic applications it may be advantageous to further slow the release of the drug and prolong the retention time of the system in the joint to enable the drug to be delivered to cartilage even more efficiently.

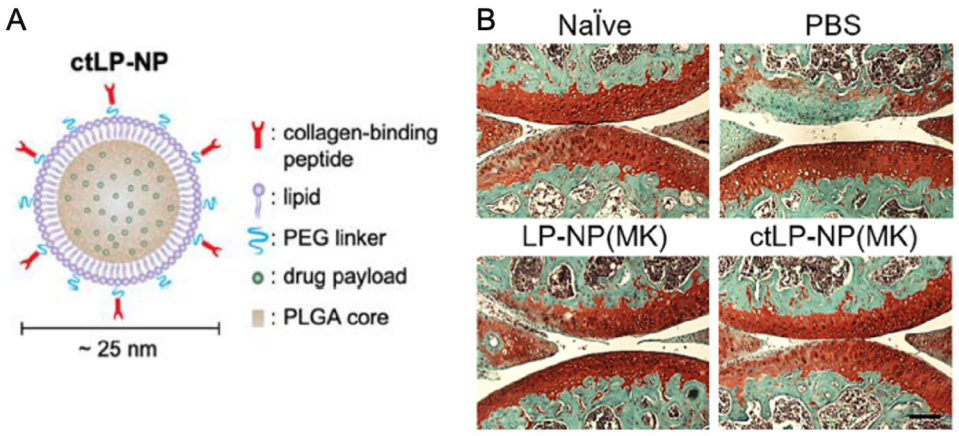

Figure 11. A) Schematic of a collagen-targeted lipid-polymer nanoparticle (ctLP-NP); B) Representative images of cartilage sections stained with safranin-O from healthy mice and collagen-induced OA mice treated with phosphate-buffered saline (PBS), lipid-polymer nanoparticles loaded with MK-8722 (LP-NP(MK), or ctLP-NP(MK). Reproduced from reference [138] with permission from Wiley, under the terms of the Creative Commons CC BY license.

3.2 Poly(lactic acid) (PLA)

PLA is another polymer that has been extensively studied for biomedical applications [140]. For example, PLA microparticles and other drug delivery depots are used clinically in the treatment of facial lipoatrophy, periodontal disease, and prostate cancer [141]. Like PLGA, PLA degrades to a metabolically processable monomer (lactic acid). Its properties depend on the lactic acid stereochemistry, with poly(L-lactic acid) (PLLA) being a semi-crystalline polymer with high tensile strength and slow degradation, and poly(D,L-lactic acid) (PDLLA, **Figure 7B**) being amorphous and exhibiting much lower tensile strength and more rapid degradation. Most recent applications in IA drug delivery have employed PDLLA.

PDLLA was used by Allémann and coworkers to study the effects of particle size on biodistribution after IA injection [142]. The particles were prepared by an emulsification method, with parameters including emulsification time and stirring speed adjusted to obtain particles with average diameters of 300 nm, 3 μm, or 10 μm, based on laser light diffraction. The fluorescent dye DiD was incorporated to enable particle tracking *in vivo*. The release of DiD was slow under *in vitro* conditions, with less than 2% released in synovial fluid over 42 days. The *in vivo*

localization of the particles, as well as particles embedded in a HA gel (0.6% w/v) for injection, was assessed in healthy mice and mice with antigen-induced arthritis (usually used to model rheumatoid arthritis) to determine the influence of inflammation on particle biodistribution. All of the particles were well tolerated, with no significant increases in inflammation scores. The fluorescence level in the joint depended on the particle size and the inflammatory status of the joint. The 300 nm particles spread from both healthy and inflamed joints, while the 3 μm particles spread from inflamed but not healthy joints, which was attributed to increased capillary permeability associated with the inflamed state. In the healthy joint cavity, 3 μm particles were retained for at least 6 weeks. The 10 μm particles were retained well in both healthy and inflamed joints. Incorporation into HA gels improved the retention of the 300 nm and 3 μm particles in the joint. Beyond the joint, low levels of particle accumulation were observed in the liver and lymph nodes. The 300 nm particles were proposed to be cleared primarily by the microvascular, 3 μm particles by both the lymphatic system and the microvasculature, and the 10 μm particles were cleared slowly by the lymphatic pathway. Overall, the authors suggested that particles of at least 3 μm in diameter should be delivered in HA to ensure retention in inflamed joints.

Allémann and coworkers incorporated crystals of the p38 MAPK inhibitor PH-797804 (PH) into PDLLA particles [143]. First, the drugs were recrystallized and then wet milled into nanocrystals with diameters between 242 and 370 nm as determined by DLS. Then, the nanocrystal-polymer particles (NPPs) were prepared by spray drying. Cy7-labeled PDLLA was incorporated to track the particles. For comparison, conventional drug-loaded microparticles were also prepared by an o/w emulsion method, and DEX was also incorporated into conventional microparticles and NPPs. The PH-NPPs had a mean diameter of 14 μm as determined by laser light diffraction, and a drug content of 32% w/w. *In vitro*, a small burst release was observed over the first 3 days, likely due to drug at or near the particles surface, but only about 20% of the PH was released from NPPs over 3 months, showing the potential of this system for sustained drug release. In a mouse adjuvant-induced arthritis model, the NPPs reduced inflammation as measured by the presence of neutrophils and granulation tissue, though they did not prevent cartilage or bone erosion. The expression of IL-1β was also suppressed. The particles were then evaluated in a murine surgical OA model. Both DEX and PH-loaded NPPs

resulted in significantly reduced OARSI scores and reduced cartilage loss. At day 63, down-regulation of the expression of IL-1β and TNFα were detected in plasma for the PH-NPPs, while DEX-NPPs only inhibited IL-1β expression. At 2 months, micrometer-sized particles were still detected in the joints, mainly in articular soft tissues.

In related work, Allémann and coworkers used the same NPP approach with KGN [144]. The KGN-NPPs had very similar sizes and drug content to the PH-NPPs. A burst release of about 20% of KGN was observed over the first day, followed by slow release of KGN, reaching about 60% over 90 days. In a murine surgical model of OA, the KGN-NPPs showed a trend towards protecting cartilage thickness compared to controls and reduced the plasma levels of VEGF, which plays a key role in chondrocyte metabolism in OA progression. On the other hand, consistent with the proposed mechanism of action of KGN, no significant effects on inflammatory cytokines were observed. A significant improvement in OARSI scores was observed for the KGN-NPPs compared to free KGN, demonstrating the benefit of the sustained release formulation. Overall, this NPP system exhibits many advantageous features of an IA drug delivery system including high drug loading, good retention in joint, slow drug release, and the potential to slow OA progression in small animal models.

3.3 Poly(ε-caprolactone) (PCL)

PCL (**Figure 7C**) is another polyester that has been used in tissue engineering and drug delivery [145]. Compared to PLGA and PLA, the degradation of PCL is much slower, often requiring 2-3 years *in vivo* [146]. Unlike PLGA and PLA, PCL does not produce an acidic environment on degradation, which can be advantageous in avoiding an undesired inflammatory response to the implanted material as it degrades [147]. Recently a couple of examples of PCL-based particles for IA delivery were reported.

Keskin and coworkers prepared PCL particles encapsulating doxycycline and CS [148]. Doxycycline (D) is a tetracycline antibiotic that has been shown to have inhibitory effects on cartilage matrix degradation [149]. The particles were prepared by an o/w emulsion procedure resulting in a mean diameter of 75 μm and a drug content of 18% w/w for the D-loaded particles and a mean diameter of 12 μm for the D and CS-loaded particles (10% w/w D, 0.3% w/w CS). The low loading of CS can likely be attributed to its high water-solubility and thus low

encapsulation efficiency during the o/w particle preparation method. *In vitro*, the particles released their cargo over 24 days, but actual percentages of cargo released were not given. *In vitro* studies were performed on chondrocytes isolated from rabbits with collagenase-induced OA, grown in agarose, and stimulated with IL-1β as a three-dimensional model of OA. Both the D-loaded, as well as D and CS-loaded particles, suppressed the release of glycosaminoglycans into the culture media at 15 and 24 days and decreased MMP levels at 24 days. In an *in vivo* rabbit model of collagenase-induced OA both particle treatments led to improved radiographic scores and Mankin-Pitzker histology scores compared to controls. Some drawbacks of the study however included a lack of a CS only particle system, which would be needed to elucidate the effects of CS versus D, and the low loading of CS in the particles.

Srivastava developed PCL particles for the IA delivery of the NSAID etoricoxib [150]. The particles were prepared by an o/w emulsion method using PVA as the surfactant. The PCL concentration and drug:PCL ratios were varied, resulting in particles with average diameters ranging from 5 – 16 μm, based on SEM, and drug loadings ranging from 2.6 – 3.5% w/w. Thermal analysis indicated that PCL retained its semicrystalline structure upon particle preparation and that the drug was incorporated in its amorphous form, dispersed in the particles. *In vitro*, about 50% of the drug was released over the first 5 days, and then release slowed, with about 90% of etoricoxib released by 20 days. Based on the known very slow degradation of PCL, the released was proposed to occur by diffusion through the particle. After IA injection of the particles into rats, plasma concentrations of etoricoxib peaked at 28 h, but were detectable over four weeks, indicating sustained release of drug. *In vivo* fluorescence imaging of rats injected IA with IR-780-loaded particles indicated that the particles were detectable in the joint for at least 4 weeks.

3.4 Poly(ester amide)s (PEAs)

Another class of polymers that has garnered increasing attention in recent years is PEAs. The presence of both ester and amide bonds in their backbones allows for both enzymatic and non-enzymatic hydrolytic cleavage, and they often undergo surface erosion rather than bulk degradation, allowing for controlled drug release and reduced concentrations of acidic species upon degradation [151]. In addition, as PEAs are synthesized by step-growth polymerization

mechanisms, they are modular in their construction, and their monomer components can be readily altered to tune their thermal, mechanical, and degradation properties [152, 153]. Furthermore, their monomers can be selected from components such as amino acids and dicarboxylic acids that are intrinsically present *in vivo*, so their degradation products can be designed to be non-toxic [154, 155]. These properties have made PEAs promising emerging candidates for IA delivery.

Timur and coworkers developed the first CXB-loaded PEA particles with the goal of achieving drug release in response to inflammation [156]. The PEA was composed of a bis-(L-leucine)-1,4-dianhydrosorbitol diester, a bis-(L-leucine)-α,ω-hexane diol-diester, sebacic acid and L-lysine benzyl ester (**Figure 12A**). This PEA was designed to be degraded by serine proteases, which are involved in inflammatory responses [157, 158]. The particles were prepared by an o/w emulsion process using PVA as a surfactant, resulting in particles with diameters ranging from about 10 to 100 μm based on DLS and SEM. *In vitro*, it was shown that fluorescein was released from PEA films that were exposed to lysates from a Hl-60 neutrophil-like cell line, a commonly used model for inflammatory cell responses [159]. The release was reduced by the addition of a serine protease inhibitor. Furthermore, elevated serine protease activity was measured in the synovial fluid and synovium conditioned media from OA patients compared to controls. After an initial burst release of about 15% of CXB, the PEA particles released the drug slowly over 80 days, showing their potential for slow release *in vivo* and the CXB delivery system reduced the levels of PGE_2, confirming an anti-inflammatory effect when injected into rats with surgically-induced OA compared to rats injected with particles containing no drug. The particles were well-tolerated in the rats, and were found entrapped in the synovium after 3 weeks. PEA degradation in the joints was monitored by resecting the joint tissues and using chromatography with mass spectrometry detection to measure the PEA content. The degradation was more rapid in OA knees compared to controls, supporting the hypothesis regarding inflammation-responsive hydrolysis of the PEA. Overall, the delivery system was very promising in terms of providing sustained and bio-responsive release in the joint. However, IA injection of the particles did not lead to reduced OA pathology in the rat model, which may be a limitation of the drug and/or the OA model.

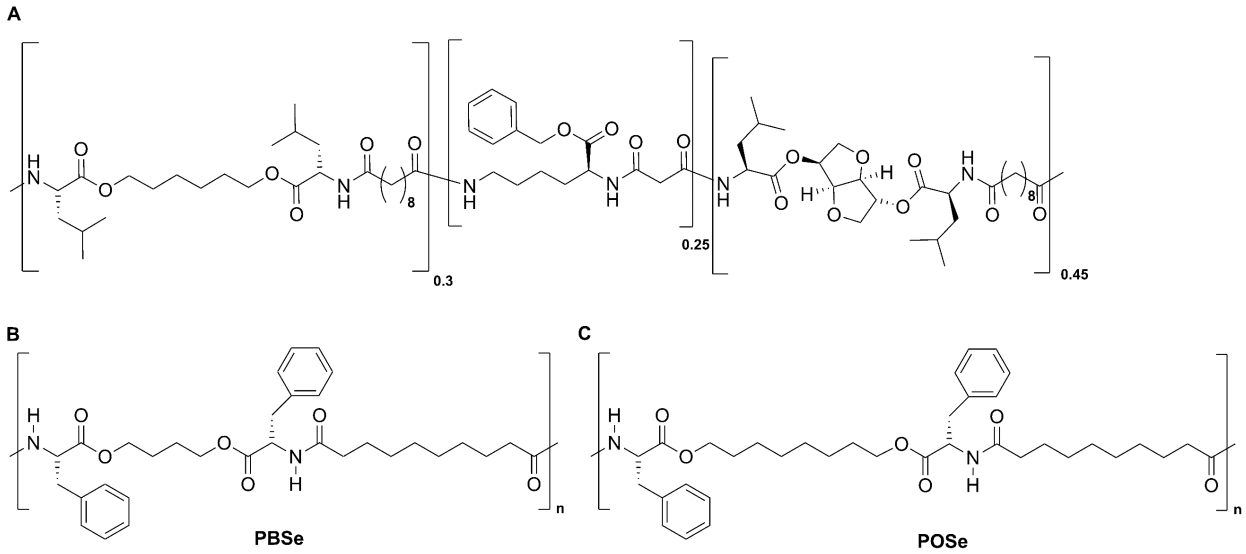

Figure 12. Chemical structures of poly(ester amide) (PEAs) used for IA drug delivery: A) Copolymer of bis-(L-leucine)-1,4-dianhydrosorbitol diester, a bis-(L-leucine)-α,ω-hexane diol-diester, sebacic acid and L-lysine benzyl ester; B) PEA composed of L-phenylalanine, sebacic acid and 1,4-butanediol (PBSe); C) PEA composed of L-phenylalanine, sebacic acid and 1,8-octanediol (POSe).

The same PEA described above (**Figure 12A**) was explored by Creemers and coworkers for the IA delivery of TA [160]. The TA-loaded particles had an average diameter of 22 μm based on SEM. The TA loading was 20% w/w, but 12% of the TA was stated to be located outside the particles, presumably adsorbed to their surfaces. *In vitro*, about 25% of the TA was released rapidly during the first couple of days, and then slow release was observed, with about 50% released in total after 60 days. In chondrocytes harvested from human patients receiving arthroplasty, and activated with TNFα, the TA-loaded PEA particles reduced the production of PGE_2 significantly compared to controls, showing their ability to suppress inflammatory responses. The PEA particles were loaded with the dye IR-780 and injected into surgically-induced OA rat knees and control rat knees. The fluorescence signal declined gradually over 70 days, showing their long-term retention in the joint. Serum TA levels were tracked and compared for free TA and TA-loaded particles injected IA. The particle system led to lower peak serum levels and detectable concentrations over a slightly longer time period (170 vs 120 h). In OA rat joints, neither free TA or the particles (empty or TA-loaded) led to any clear effects on cartilage integrity, but the TA-loaded PEA particles led to decreased synovial inflammation. Overall,

these results confirm the potential of the PEA particle delivery system to provide sustained drug release *in vivo* without an adverse host response, and that the TA delivery system in particular may be useful in reducing inflammation-associated pain for OA patients.

Gillies and coworkers also investigated PEA particles for the delivery of potential OA therapies to joints. In the initial study, two different PEAs were compared [161]. One PEA was composed of L-phenylalanine, sebacic acid and 1,4-butanediol (PBSe, **Figure 12B**), while the other contained 1,8-octanediol instead of 1,4-butanediol (POSe, **Figure 12C**). The particles were prepared by an o/w emulsion process using PVA as a surfactant, and CXB was loaded at about 20% w/w. The drug-loaded PBSe and POSe particles had average diameters of 1040 and 640 nm respectively based on SEM. Most importantly, the small structural difference between PBSe and POSe resulted in an important change in their thermal properties, with CXB-loaded PBSe particles having a glass transition temperature (T_g) of 41 °C and the analogous POSe particles having a T_g of 30 °C. These thermal data indicate that the PBSe particles would be in a glassy state at 37 °C, close to their transition, whereas the POSe particles would be in a rubbery state. Tensile testing was performed on CXB-loaded PBSe and POSe immersed in water at 37 °C and both materials had Young's moduli in the range of the modulus for articular cartilage (0.4 – 0.8 MPa). *In vitro*, the POSe particles released CXB more rapidly, with about 80% released over 60 days, while the PBSe particles released only about 30% over the same time period, with no burst release. PBSe particles were still observed by SEM after 60 days, while POSe particle were largely destroyed in the first 7 days, presumably due to their rubbery state. Based on their more promising profile, the CXB-loaded PBSe particles were injected into the knees of healthy sheep. The particles were well tolerated by the sheep and were found in the synovial membrane.

The PBSe particle delivery system was also applied by Gillies and coworkers to the encapsulation of the PPARδ antagonist GSK3787 [162]. The particles were prepared by a similar o/w emulsion method to that used for CXB, but it was necessary to reduce the drug loading to 8% w/w to obtain particles. Thermal analysis suggested that the reason for this limit was that GSK3787 was phase-separated from the PEA, whereas CXB was homogeneously distributed throughout the PEA phase. The GSK3787-loaded particles had an average diameter of 580 nm based on SEM. In this work, the compression moduli of individual GSK3787-loaded particles were measured by atomic force microscopy, and the average modulus was 2.8 MPa, a bit higher than that of articular cartilage. *In vitro*, GSK3787 was released slowly from the particles, with

11% released over 30 days, and no burst release was observed. The drug, empty particles, and drug-loaded particles exhibited low cytotoxicity in immature murine articular cartilage (IMAC) cells. *Ex vivo* injections of IR-780-loaded particles into murine knee joints showed that the particles were still observable in the joints after 7 days. Overall, the delivery system is promising, but further research will be needed to assess its efficacy in OA models *in vivo*.

3.5 Thermoresponsive polymers

Thermoresponsive polymers have been extensively studied for biomedical applications [163]. In particular, poly(*N*-isopropylacrylamide) (pNIPAM, **Figure 13A**) exhibits a lower critical solution temperature (LCST) of about 32 °C, where it changes from a water-soluble hydrated state to a collapsed or aggregated state, driven by the entropically-favorable release of water molecules [164, 165]. This transition has been used to induce gelation and self-assembly of polymer systems for IA drug delivery.

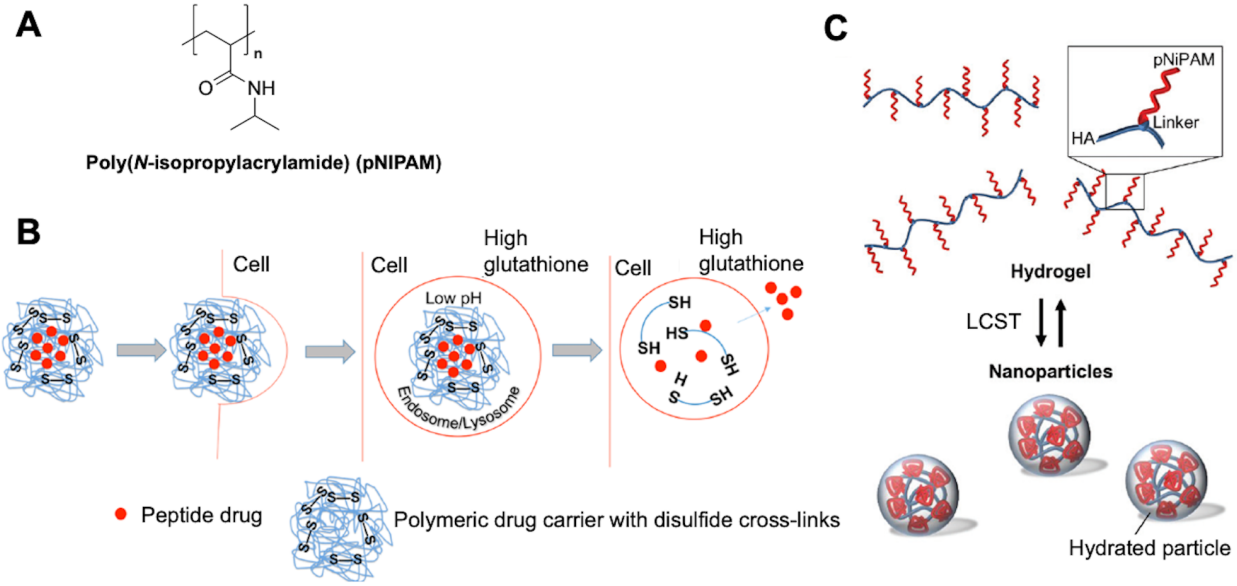

Figure 13. A) Chemical structure of pNIPAM; B) Particles designed to release the peptide KAFAK in response to elevated glutathione concentrations (Reproduced with permission from reference [166]. Copyright 2015 American Chemical Society); C) pNIPAM-hyaluronic acid (HA) graft copolymer conjugate that self-assemblies into nanoparticles above the lower critical solution temperature (LCST) to prolong the lifetime of HA on the joint (Reproduced with permission from reference [167]. Published by the Royal Society of Chemistry).

Panitch and coworkers have investigated pNIPAM-based particles for the delivery of anti-inflammatory peptides [166, 168-171]. The team developed a 23-mer cell-penetrating peptide, referred to as KAFAK, that inhibits mitogen-activated protein kinase-activated protein kinase 2 (MK2), with the aim of reducing the expression of pro-inflammatory cytokines such as IL-1, TNFα, and IL-6 [172]. However, a delivery system was needed to protect the peptide from enzymatic degradation and increase its release time *in vivo*. In their early work, they prepared nanogels from NIPAM, and 2-acrylamido-2-methyl-1-propanesulfonic acid (AMPS) as monomers, as well as *N*,*N'*-methylenebisacrylamide (MBA), and *N*,*O*-dimethacryloylhydroxylamine (DMHA) as crosslinkers [168]. The cationic KAFAK peptide was loaded into the nanogels through ionic complexation, facilitated by AMPS, below the LCST. DMHA degrades hydrolytically above pH 5. KAFAK was released over 24 h from the different systems, with higher release from the particles containing degradable DMHA. KAFAK was unable to completely release from the nondegradable particles.

The KAFAK-loaded particles were later improved through the incorporation of PEG to impart stealth, and disulfide crosslinks to allow for selective degradation of the particles at enhanced rates under the conditions of low pH and elevated glutathione concentrations in intracellular compartments such as endosomes and lysosomes after cell uptake (**Figure 13B**) [166]. The resulting particles contained about 30% w/w KAFAK and were about 220 nm in diameter. The particles were stable in the absence of reducing agents, but were degraded over 48 h when the dithiothreitol (DTT) was added. The diameters of the particles decreased continually as the temperature was raised from 20 – 50 °C, due to chain collapse of pNIPAM. In addition, the presence of DTT or low pH (pH 4.0) induced the release of about 25-30 % of the KAFAK over 96 h, whereas in the absence of these stimuli at pH 7.4 only about 7% of the KAFAK was released. Considering the incorporation of the peptide by ionic interactions and the fact that more complete release could be achieved from particles without anionic AMPS, the low levels of KAFAK release are rather surprising, and suggest that irreversible aggregates composed of peptide and the pNIPAM-AMPS polymer may form. As pNIPAM is considered a non-degradable polymer, it would not be expected to break down over the timeframe of the experiment to release the peptide. *In vitro* studies in RAW 264.7 murine macrophages showed that the KAFAK-loaded PEGylated reduction-sensitive particles inhibited the production of IL-6

and TNFα more effectively than the free peptide, as the free peptide was presumably degraded enzymatically in the presence of serum, while the particles protected the peptide. The authors also demonstrated the uptake of these particles into primary bovine chondrocytes and showed that they colocalized with endolysosomal compartments. Furthermore, they showed that fluorescein-labeled particles exhibited greater penetration through inflamed, aggrecan-depleted bovine cartilage explants compared to health cartilage. The particles were also able to suppress IL-6 secretion in these explants, whereas free KAFAK was not effective due to its degradation.

Subsequently, Panitch and coworkers addressed the challenge of limited KAFAK release through the development of hollow PEGylated pNIPAM particles [170]. First, degradable particle cores were prepared from NIPAM and *N*,*N'*-bis(acryloyl)cystamine (BAC) by free radical precipitation polymerization, then the shells were prepared from NIPAM, MBA, PEG-acrylate, and AMPS in the presence of sodium dodecyl sulfate. The cores were subsequently degraded using DTT, and then the peptide was loaded into the shells of the hollow particles through ionic interactions. The particles had an average diameter of about 290 nm at 25 °C, which was reduced to 240 nm at 37 °C, due to the LCST of pNIPAM. The KAFAK loading was 50% w/w, which was higher than for the solid particles described above, likely to their lower peptide diffusion barrier during loading of the hollow compared to solid particles. The hollow particles released 50% of the loaded peptide over 4 days *in vitro*. The particles were taken up by RAW 264.7 macrophages and were found in endolysosomal vesicles at 24 h. They were demonstrated to penetrate effectively into aggrecan-depleted bovine cartilage *ex vivo*, and significantly reduced IL-6 production in these explants. In recent work, Panitch and coworkers improved the hollow pNIPAM particles by lowering the crosslink density to allow the incorporation of the peptide YARA, a more specific MK2 inhibitor [171]. They also incorporated the degradable crosslinker into the shell, allowing it to degrade, facilitating the release of YARA. Overall, these results show the potential of these peptide delivery systems. An important next step will be their evaluation in an *in vivo* OA model.

Allémann and coworkers conjugated pNIPAM to HA with the goal of increasing the residence time of HA injected into the joint (**Figure 13C**) [167]. The pNIPAM chains were grafted onto HA using a strain-promoted azide-alkyne cycloaddition reaction. At physiological temperature, the copolymers self-assembled to form particles with diameters ranging from 130 –

240 nm based on DLS. The formulations were injectable at room temperature, and when self-assembled into particles imparted increased resistance of the HA to enzymatic degradation. The residence time of fluorescently-labeled particles exceeded 21 days, whereas HA alone diffused from the injection site during the first day. In a mouse surgical model of OA, the particles protected cartilage and reduced pro-inflammatory cytokines compared to controls. It was also suggested that the hydrophobic pNIPAM cores of the assemblies could potentially be used to encapsulate and delivery drugs in future studies.

pNIPAM-based particles have also been employed in OA delivery systems designed to simultaneously provide enhanced lubrication and thermoresponsive drug delivery [173] (**Figure 14**). Xu, Wang, Zhang, and coworkers prepared nanogels from *N*-isopropylacrylamide and 2-methacryloyloxyethyl phosphorylcholine (MPC) by a w/o emulsion polymerization using methylene bisacrylamide (MBA) as a crosslinker. The resulting particles had a diameter of about 220 nm at 25 °C, based on DLS, and the diameter gradually decreased to 145 nm as the temperature was increased to 50 °C. The NSAID DCF was loaded into the particles. At 25 °C they released 73% of the drug, whereas at 37 °C, 88% of drug was released over 72 h. Physiologically, the release rate at 37 °C would be the most relevant, so the system would be most useful for the relatively rapid release of therapeutics. The lubrication properties of the particles were investigated, and it was found that the coefficient of friction decreased as the content of MPC monomer was increased, up to about 20%, and also as the concentration of the particles increased, up to 20 mg/mL. The particles reduced wear between polytetrafluoroethylene (PTFE) and silicon, with their lubricating properties were attributed to the hydration layer associated with the charged groups on MPC, which mimics the behavior of phosphatidylcholine lipids. *In vitro* studies in primary murine chondrocytes showed that the particles had low cytotoxicity. In addition, the particle led to increased expression of aggrecan and decreased expression of MMP13 and ADAMTS5. In a related biomimetic approach, the same group grafted MPC to mesoporous silica nanospheres by photopolymerization [174]. These particles were also effective in enhancing lubrication and providing sustained release of DCF over 72 h. In a rat surgical model of OA, the DCF-loaded particles with grafted polyMPC led to the least cartilage damage, as indicated by histological evaluation, and a significant reduction in OARSI score compared to controls. These results were attributed to a down-regulation of catabolic

enzymes and up-regulation of anabolic factors arising from both the drug and lubricating properties. Overall, this system warrants further study as a potential OA therapy.

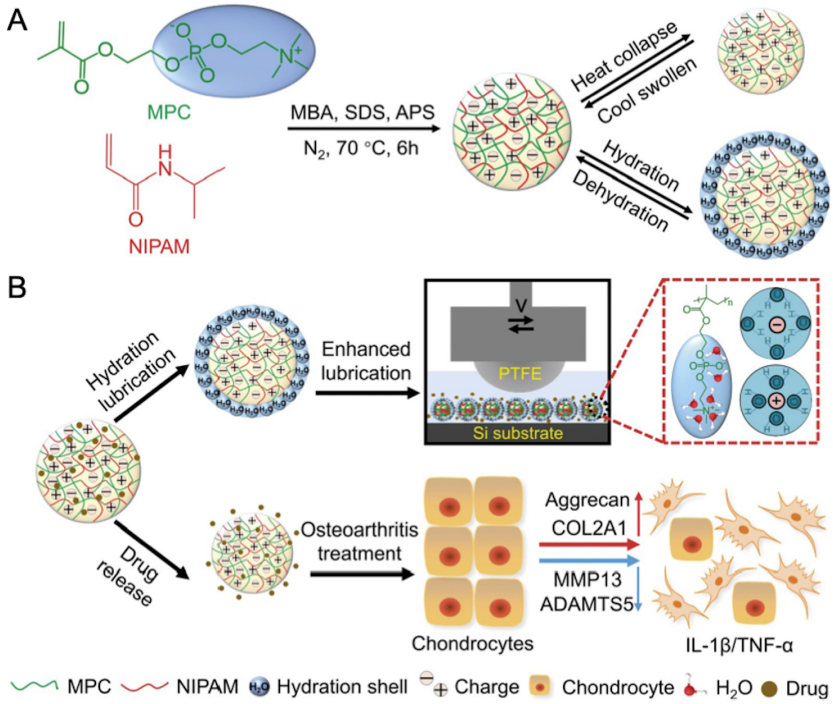

Figure 14. Schematic of a delivery system containing zwitterion polymer for lubrication, pNIPAM for thermoresponsiveness, and drug loading capabilities. SDS = sodium dodecyl sulfate; APS = ammonium persulfate. Reproduced from reference [173] with permission from Wiley, under the terms of the Creative Commons CC BY license.

pNIPAM has also been used by Ni, Kong, Zhao, and coworkers for the preparation of biomimetic inverse opal-structured particles loaded with both HA and DCF [175]. The particles were prepared by first self-assembling silica nanoparticles using a microfluidic device to generate colloidal crystal beads with interconnected nanovoids. These beads were then immersed in pNIPAM pre-gel, allowing the polymer to diffuse into the beads. The pNIPAM was crosslinked photochemically, and the outer hydrogel and the silica were removed. Subsequently, methacrylate-functionalized HA and DCF were loaded into the nanopores and the HA was crosslinked. The resulting particles were about 200 μm in diameter and released the DCF over

about 10 days, with slightly faster release at 39 °C than at 37 °C. The particles were well tolerated by human chondrocytes *in vitro*. In a rat surgical model of OA, the drug-loaded lubricating particles led to the most reduced cartilage damage and lowest OARSI scores compared to control groups, as well as the highest aggrecan and collagen 2 expression. These results the suggest the promise of this particle system for OA and reaffirm the potential benefits of combining drugs and lubricating properties in a single delivery system.

3.6 PVA

A Phase 2 clinical trial recently began to evaluate the safety, efficacy, and pharmacokinetics of EP-104AR in patients with knee OA. The system is composed of crystals of the corticosteroid fluticasone propionate, coated with a semipermeable shell of heat-treated PVA, resulting in particles with mean diameters in the range of 50 – 100 μm [176]. To determine the pharmacokinetic profile of EP-104AR, 0.6 mg and 12 mg doses were injected IA into Beagle dogs. The injections were well tolerated based on histopathology. At the lower dose, fluticasone propionate was not quantifiable in the plasma. At the higher dose, the peak concentration was measured one day post-injection and declined thereafter. After this time, many of the plasma concentrations were below the limit of quantitation, but crude estimates suggested a half-life of about 45 days for fluticasone propionate in plasma. In synovial fluid, the highest concentrations of drug were measured at the first assessment point of 7 days, and decreased with a half-life of about 11 days. All but one of the animals receiving the high dose had quantifiable drug concentrations at day 60 in the synovial fluid. In addition, quantifiable concentrations of the drug were detected in the cartilage of the dogs through day 60 and the half-life in cartilage was estimated to be about 14 days. This study showed the potential for EP-104AR to provide safe and prolonged delivery of the corticosteroid, which may relieve synovitis-associated pain and inflammation in OA patients. The current clinical study will evaluate the difference between the change from baseline to 12 weeks of the WOMAC pain subscale for EP-104AR compared to a vehicle control as its primary outcome measure. However, like other steroids, this steroid-based therapeutic would not be expected to alter the long-term disease course of OA.

3.7 Amphiphilic copolymer assemblies

It is well established in the polymer field that amphiphilic polymers tend to assemble in aqueous solution into organized structures [177, 178]. This spontaneous process is driven by the hydrophobic effect, where hydrophobic molecules, or portions of molecules aggregate to exclude water molecules, avoiding the entropically unfavorable organization of water molecules around a hydrophobic solute. There are many ways in which amphiphilicity can be introduced to polymers, including the preparation of diblock or triblock copolymers where the different blocks have different hydrophilicity, as well as random copolymers, graft copolymers and other architectures (**Figure 15**). The size and morphology of the resulting assemblies can be tuned based on the structure of the copolymer as well as the conditions under which self-assembly is performed. There are several recent examples involving the preparation of amphiphilic copolymer particles for the IA delivery of drugs to potentially treat OA.

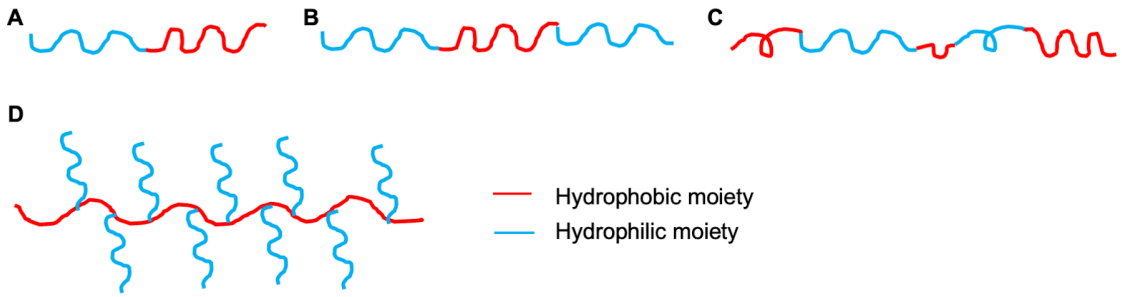

Figure 15. Schematic illustration of an amphiphilic A) block copolymer; B) triblock copolymer; C) random copolymer; D) graft copolymer.

García and coworkers explored self-assembled polymer nanoparticles presenting the IL-1 receptor antagonist IL-1Ra [179, 180]. The amphiphilic polymer was 20 kg/mol poly(2-hydroxyethyl methacrylate) (pHEMA) functionalized on its pendent hydroxyl groups with nicotinyl chloride (**Figure 16A**) [179]. The polymers were self-assembled concomitantly with protein complexation, leading to particles with average diameters of 200 – 900 nm depending on the polymer:protein ratio and the identity of the particular protein. Using BSA with a near-IR fluorophore as a model protein, the role of particle size on retention time in rat joints was studied. Whereas free BSA had a half-life of only 0.6 days, BSA complexed to 500 and 900 nm particles had half-lives of 1.9 and 2.5 days respectively, with about 30% of BSA retained at 14 days for the 900 nm particles. These results suggested that despite the protein immobilization

being non-covalent, the BSA likely remained complexed to the particles. Next, IL-1Ra was complexed at 1:1 and 3:2 protein:polymer ratios, leading to particles with average diameters of 320 and 610 nm respectively, based on DLS and SEM. The particles were non-cytotoxic to RAW 264.7 macrophage cells. In addition, the particles inhibited IL-1β-stimulated NF-κB activation in a cell line expressing luciferase in response to NF-κB activation, showing that IL-1Ra retained biological activity after complexation to the polymer assemblies. Overall, the bioactivity of the complexed IL-1Ra and enhanced retention of the self-assembled polymer-protein particles suggest the potential for this new system in the treatment of OA, but to the best of our knowledge no further studies on its *in vivo* activity have been reported.

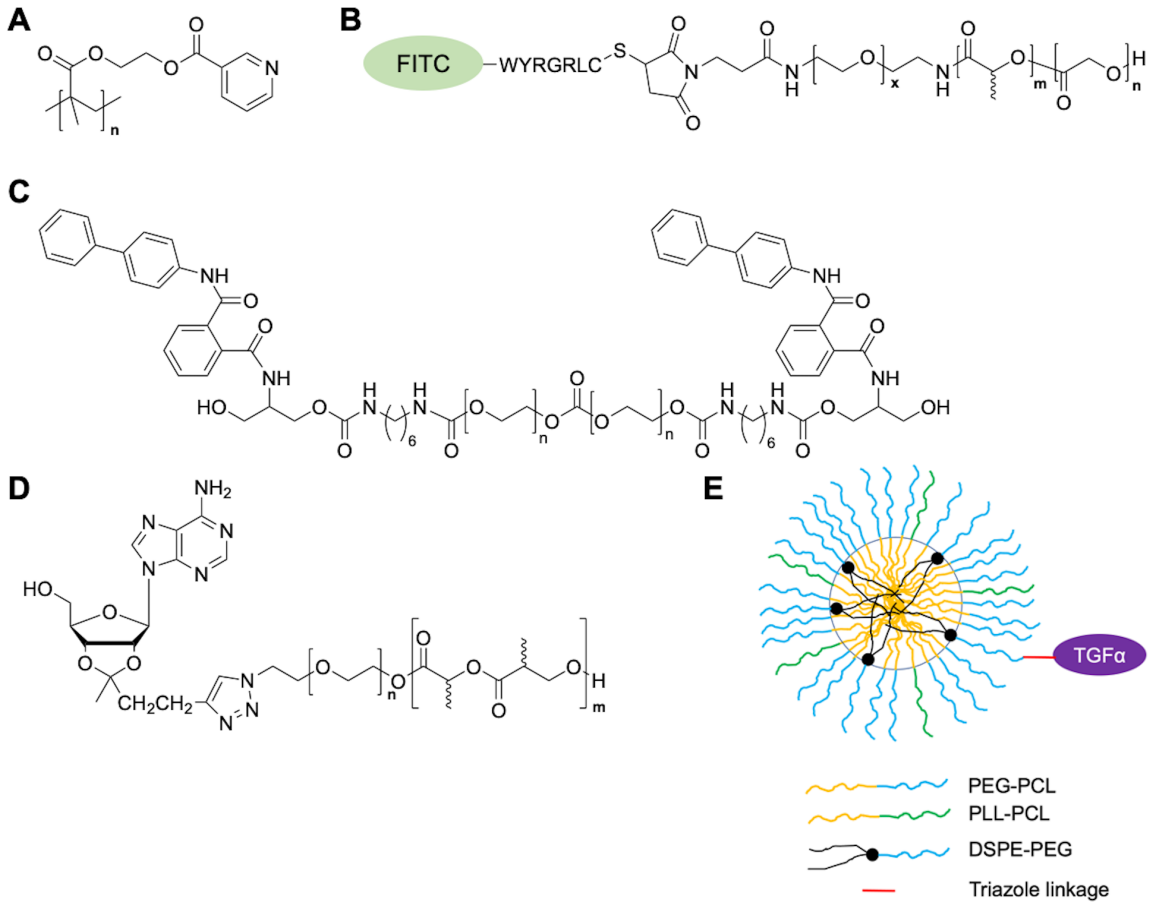

Figure 16. A) Chemical structure of pHEMA functionalized with nicotinyl chloride; B) PEG-PLGA functionalized with a FITC-labeled peptide to target collagen type 2; C) KGN-functionalized polyurethane; D) Adenosine-functionalized PLA-PEG block copolymer; E)

Schematic of TGFα-functionalized micelles composed of PEG-PCL and PEG-PLL block copolymers and PEG-lipid (DSPE).

Lo and coworkers explored the potential for the short collagen type 2 binding peptide sequence WYRGRL to provide targeting of PEG-PLGA nanoparticles to cartilage tissue [181]. The particles were prepared from a mixture of 1:9 maleimide-functionalized-PEG-PLGA:methoxy-terminated-PEG-PLGA using a double emulsion technique (**Figure 16B**). FITC-tagged WYRGRLC peptide was then conjugated onto the NP surface via the cysteine thiol group. The average diameter of the particles was 256 nm, as measured by DLS. Polyacrylamide gel electrophoresis results showed that the FITC moiety did not disrupt the binding of the peptide to type 2 collagen. *In vitro*, the peptide-functionalized particles bound to human chondrocytes whereas particles functionalized with a random peptide sequence did not, based on fluorescence microscopy. The targeted particles also bound to cartilage tissue sections *ex vivo*. This study provided support for potential targeted delivery of the particles to cartilage. However, further studies will need to be performed to assess the ability of the particles to release drugs in a controlled manner and to exhibit sustained retention and cartilage penetration *in vivo*.

KGN-conjugated polyurethane particles were reported by Fan and coworkers [182]. Amphiphilic polyurethanes were synthesized via step-growth polymerization of PEG, *N*-butyloxycarbonyl (BOC)-protected serinol, and hexamethylene diisocyanate, followed by removal of the BOC protecting groups (**Figure 16C**). KGN was then conjugated to the resulting pendent amines by a carbodiimide coupling. Particles were formed upon dialysis of the conjugation product against water, followed by lyophilization. Based on TEM and DLS, the resulting particles had an average diameter of about 25 nm. *In vitro*, about 20% of KGN was released over 15 days, and then it reached a plateau for a further 15 days. As amide bond hydrolysis to release KGN would not be expected to exhibit such a release profile, these results raise the question of whether the observed release corresponded to non-covalently bound drug. *In vitro* studies with primary rat chondrocytes showed that the particles were non-toxic at concentrations leading to the release of up to 100 nM of KGN based on the release studies and that they did not induce pro-inflammatory activity in these cells. In a rat surgical model of OA, the particles (administered every 3 weeks) led to less extensive cartilage degradation and lower OARSI scores at the 12 week end point than control non-treated rats. It was proposed that the

cationic charge of the particles, resulting from the non-functionalized amines, as well as their small size, facilitated their penetration into the cartilage matrix, providing an intra-cartilage release of KGN.

Ulman, Cronstein, and coworkers studied adenosine-functionalized PLA-PEG block copolymer nanoparticles [183]. It has been proposed that extracellular adenosine is an important homeostatic mechanism for chondrocytes and that loss of adenosine receptor-mediated homeostasis may contribute to OA development. Liposomal suspensions of adenosine prevented the development of OA, but did not exhibit sufficiently sustained release, so the authors proposed that covalent conjugation of adenosine to a polymeric nanocarrier would allow more effective and sustained activation of the adenosine receptor. The conjugates were prepared by azide-alkyne click reactions between an azide on the PEG terminus and adenosine functionalized with an alkyne at either the 3',4'-OH groups, 5' OH group, or 6-NH_2 group. Both 400 and 2000 g/mol PEG blocks were studied. The particles were prepared by an o/w emulsion process using poloxamer 188 as a surfactant, resulting in average diameters of 129 – 144 nm based on DLS. In RAW 264.7 macrophages, only the particles prepared from the 3',4'-OH conjugate with a 2000 g/mol PEG block (**Figure 16D**) stimulated the adenosine receptors. In primary murine chondrocytes, these nanoparticles reduced the IL-1β-stimulated expression of IL-6, MMP-13, and collagen 10. The effect was reversed by a receptor antagonist. IA injection of the adenosine-functionalized particles into the knees of rats reduced swelling, decreased the OARSI score, and prevented cartilage loss in a surgical OA model compared to controls. Overall, these particles show promise for OA treatment.

Recently, Cheng, Qin, and coworkers used polymer micelles to deliver TGFα [184], a ligand capable of activating the epidermal growth factor receptor (EGFR), which is implicated in OA progression [185] (**Figure 16E**). The micelles were composed of PEG-PCL, poly(L-lysine) (PLL)-PCL, and an azide-functionalized PEG-lipid. TGFα was conjugated to the micelle surface using a strain-promoted azide-alkyne cycloaddition reaction. The particles had a diameter of 26 nm based on DLS. The cationic surface charge imparted by the PLL-PCL enhanced cartilage penetration 5-fold over 6 days compared to particles without PLL-PCL. In addition, the particles led to enhanced retention of TGFα in mouse knee joints over 28 days compared with the free protein. In a mouse surgical model of OA, administration of the TGFα micelles led to elevated EGFR activity in cartilage and reduced cartilage damage based on histological analysis. In

addition, the micelles inhibited the thickening of the subchondral bone plate based on three-dimensional micro-computed tomography, and reduced synovitis and pain. Overall this combination of drug and delivery system shows promise for further translation as a potential OA therapy.

3.8 Dendrimers

Dendrimers are a unique class of synthetic polymers that is composed of branching monomers. These monomers are incorporated onto a multivalent core, layer-by-layer, through step-wise synthesis, leading to well-defined branched macromolecules [186]. The dendrimer generation refers to the number of concentric layers surrounding the core. Compared to linear polymers, which have two end groups that do not usually impact substantially the properties of the polymer, dendrimers have many peripheral groups that dominate their properties. In addition, as the number of peripheral groups increases exponentially at each generation, the density of peripheral groups also increases, leading to spherical, globular conformations. Dendrimers have been of particular interest for biomedical applications because they can be synthesized with very reproducible molar masses, and their surface groups can be easily functionalized to introduce multiple drugs, imaging agents, or moieties to control their solubility, toxicity, and tissue targeting [187, 188]. So far, only one class of dendrimers, referred to as polyamidoamine (PAMAM) dendrimers (**Figure 17A**) has been explored for IA delivery.

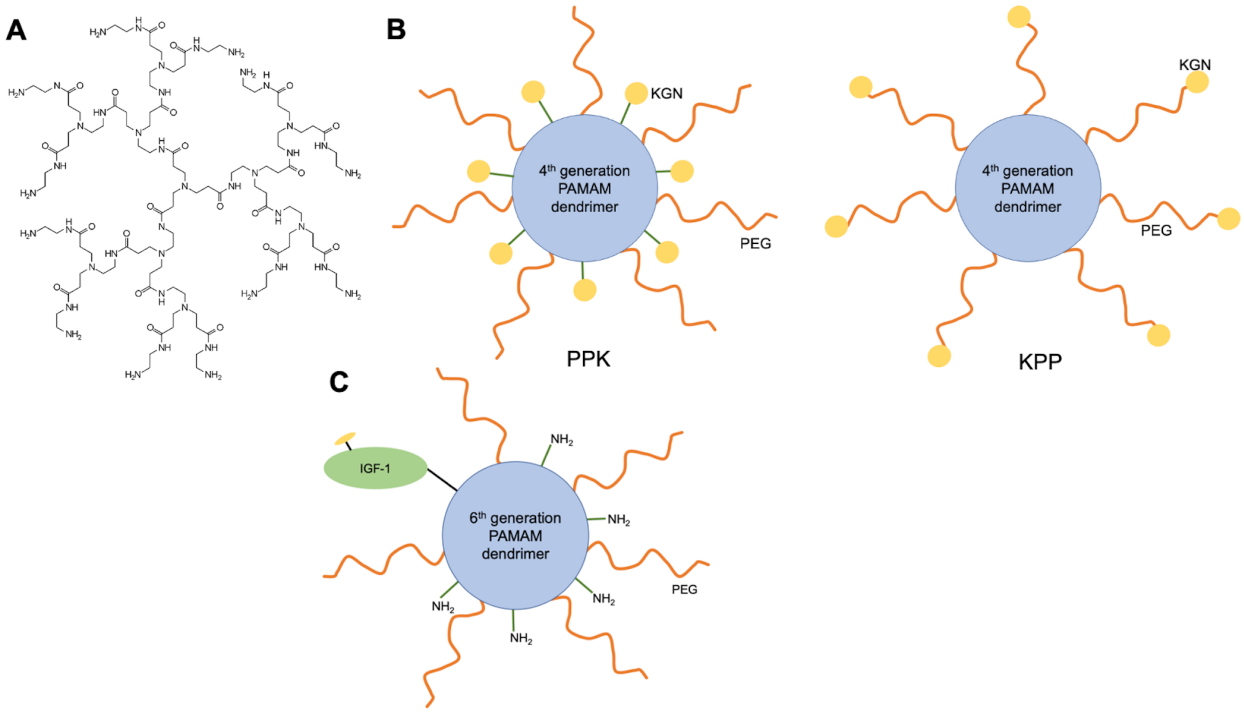

Figure 17. A) Chemical structure of a PAMAM dendrimer; B) Schematics of PAMAM dendrimers conjugated to KGN either at the dendrimer surface or at the termini of PEG chains; C) Schematic of a PAMAM dendrimer conjugated to PEG and IGF-1. In B and C the number of PEG chains and amines are just representative and do not reflect the numbers of these groups in the actual structure.

Chang, Chen, and coworkers conjugated KGN to PAMAM dendrimers with the goal of inducing chondrocyte differentiation of MSCs [189]. First, PEG was conjugated to about 20 of the dendrimer's 64 peripheral amines, then KGN was conjugated to about 10 of the remaining amines to give the conjugate called PPK (**Figure 17B**). Alternatively, KGN was first conjugated to one end of a H_2N-PEG-NH_2, and then the other end was conjugated to the dendrimer amines using a linker. Additional PEG chains were added to achieve similar overall PEGylation to PPK, giving a second conjugate called KPP with the drug on its periphery. Both dendrimers had average diameters of about 35 nm based on DLS, positive zeta-potentials, and were non-toxic to bone marrrow MSCs up to at least 50 μM equivalent of KGN. Treatment of the MSCs with 1 μM equivalent of KGN led to upregulated expression of chondrogenic marker genes and increased levels of collagen type 2 and aggrecan for the free drug and both dendrimers compared to untreated controls. Overall, KPP was more effective in inducing chondrogenic differentiation,

because the PEG may have shielded the KGN in PPK. The PEGylated PAMAM dendrimers were labeled with Cy7, injected into the joints of healthy rats, and their residence time was compared to that of free Cy7 using *in vivo* imaging. Most of the signal for the free Cy7 disappeared within the first 24 h, whereas 60% of the fluorescence of the Cy7-labeled dendrimer remained after 3 days. Similar results were also obtained in rat joints with IA induced by papain injection, with fluorescence from the dendrimers still detectable at 3 weeks. The retention of the dendrimers in the joint was attributed to their cationic charge allowing for binding to negatively charged species in the synovial fluid or to aggregation and subsequent macrophage uptake, providing a depot for prolonged release.

Hammond and coworkers studied cationic PAMAM dendrimers for IA delivery with the goal of achieving penetration into cartilage tissue, to effectively deliver IGF-1 to chondrocytes [190] (**Figure 17C**). Fourth and sixth generation dendrimers, with 64 and 256 peripheral amino groups respectively, were PEGylated at 0 – 60% of their amines. Fluorescently-labeled IGF-1 was conjugated via a thiol-maleimide linkage and shown to retain biological activity equivalent to that of free IGF-1. Cartilage uptake of the dendrimers was measured after incubation with bovine cartilage disks for 24 h. All of the dendrimers preferentially partitioned into anionic cartilage tissue, presumably due to electrostatic interactions due to their cationic charges. PEGylation decreased this uptake. On the other hand, PEGylation enhanced the viability of CHON-001 chondrocytes incubated with the dendrimers for 48 h. To balance these effects, a generation four PAMAM with 35% of its amines PEGylated and a generation six PAMAM with 45% of its amines PEGylated were selected for further study, as they provided high cartilage uptake, while retaining 100% cell viability at 10 μM of dendrimer. The dendrimer conjugates and free IGF-1 were injected IA into rat knees and the fluorescence within joints was monitored for 1 month using *in vivo* imaging. While free IGF-1 had a half-life of only 0.4 days, the generation four and six dendrimer conjugates had half-lives of 1 day and 4 days respectively. At 6 days, IGF-1 was detected throughout the femoral cartilage. The sixth generation PAMAM-IGF-1 conjugate was evaluated in a surgical rat model of OA. Compared to untreated rats and those treated with free IGF-1, rats treated with the dendrimer exhibited reduced cartilage degradation, reduced synovial inflammation, and reduced osteophyte burden. Overall, this study demonstrated how the size and peripheral functionalization of dendrimers could be successfully used to tune their toxicity and cartilage penetration, enhancing the efficacy of a potential OA

therapeutic by more effectively delivering it to chondrocytes. The PAMAM carrier can potentially be conjugated to other drugs, including both small molecules and proteins.

4. Challenges and future perspectives

Thus far, a wide array of polymers ranging from biopolymers to synthetic polymers, and hybrids thereof have been investigated for the preparation of particles for IA drug delivery to treat OA. However, in the context of polymer chemistry, where nearly an unlimited array of structures are possible and thousands of different polymers have been reported, the number of polymers that have been investigated is actually quite limited. Many more examples of polymers with "smart" functions such as stimuli-responsive drug release have been reported for anti-cancer drug delivery [191-193]. Researchers and companies interested in translating discoveries to the clinic in a timely manner often use established polymers such as PLGA, which have received regulatory approval previously for other applications. This is a valid approach, but the consequence is that promising emerging polymers may be overlooked and opportunities lost. In this context, it is important for both academic teams and industry to investigate new materials, and to perform clinical trials on these materials, with the goal of achieving regulatory approval for a greater diversity of polymer platforms.

One aspect that requires careful consideration for any injectable polymer is its biodegradability. Of the biopolymers investigated for IA delivery over the past 5 years, polysaccharides such as chitosan, HA, and CS likely degrade most rapidly [194-196], while silk fibroin degrades more slowly [103, 104]. Of the synthetic polymers discussed in this review, polyesters such as PLGA and PDLLA degrade more rapidly, while PCL and PEAs degrade more slowly [140, 141, 146]. Ultimately, the desired timeframe for polymer degradation will depend on the drug's desired release profile. Synthetic polymers, such as pNIPAM, with carbon-carbon bonds throughout their backbones, would not be expected to degrade at appreciable rates *in vivo*, and would need to be excreted through renal or hepatic routes after leaving the joint to avoid accumulation over the long term. This lack of degradability could be a hindrance to clinical translation, as the long-term fate and effects of such materials after IA injection remains unknown.

The mechanical properties of particles injected into the joint are important, yet they have received little attention to date. Suspensions of drug crystals, including TAcs, are injected

routinely in clinical practice. However, the deposition of crystals such as calcium pyrophosphate in the synovium can lead to crystalline arthritis [197]. The reasons for crystal tolerance versus reactivity are not well understood and should be considered in the development of any crystallizing drug/delivery platform. The moduli of polyesters like PLGA, PDLLA, and PCL range from about 300 MPa to about 2 GPa [198, 199], much higher than that of joint tissues other than bone [200]. Therefore, it seems reasonable to be concerned that particles composed of polymers like PLGA could cause mechanical irritation in the joint. Particles can activate innate immune mechanisms, leading to intense inflammation *via* toll-like receptor binding of particles acting as danger-associated molecular patterns (DAMPs) [201]. This effect may be mitigated by the delivery of a corticosteroid or NSAID, as these are commonly used treatments for synovitis [197], but as the field moves toward the delivery of new disease-modifying drugs, it will be critical to ensure that the delivery system does not trigger joint inflammation.

Of the particle systems described in this review, the drug release times varied considerably, ranging from hours to months. In general, assemblies composed of hydrophilic polymers such as chitosan tended to release drugs rapidly *in vitro*, presumably due to enhanced water penetration [70, 71, 80]. On the other hand, the encapsulation of drugs into more hydrophobic polymers like PLGA [112, 115], PDLLA [143], and PEAs [156, 160-162] can lead to the release of drug over months. Nevertheless, even particles that released drug over months *in vitro* exhibited burst-type release profiles *in vivo*, with high and then rapidly decreasing concentrations of drug in the joint, suggesting there are additional factors such as enzymes and trafficking of the particles out of the joint that occur *in vivo* [114, 176]. Engineering the release profile of a drug from the delivery system is a complex issue. The concerns regarding a high initial burst release of drug include the potential for high local drug concentrations to lead to off-target effects in the joint or systemic side effects, resulting from high plasma drug concentrations. Aside from potential side effects, sustained low concentrations of highly potent drugs in the joint after an initial burst release may be sufficient for therapeutic effects. In other cases, these low concentrations may be insufficient. In addition, depending on the mechanism of action of the drug, the clinical benefits may long exceed the half-life of the drug, while in other cases, sustained drug concentrations at a critical threshold may be needed. Overall, delivery systems capable of releasing drugs over extended time periods, and even in response to disease flares, as recently demonstrated for hydrogels [202, 203] may be beneficial. On the other hand,

for safety considerations clinicians may also want to "turn off" drug release if necessary. Such abilities have been engineered into genome editing approaches for OA [204], but may be challenging to incorporate into delivery systems for small molecule drugs.

A further challenge is a lack of ability to correlate *in vitro* drug release profiles with *in vivo* release. It would be beneficial to measure drug release under more biologically relevant conditions *in vitro*. For example, enzymes could be added to the release media to mimic proteolytic degradation as suggested by Timur and coworkers [156]. However, even these approaches may be insufficient. *In vivo* animal models are likely the best pre-clinical correlate, but perhaps *in vitro* organ culture systems and/or organ-on-a-chip technologies could play a role in future early stage research.

Particle size and charge have been investigated to some extent, but remain important aspects for further study. To reach drug targets in chondrocytes, penetration through cartilage, a dense network of collagen fibrils and glycosaminoglycans, remains a challenge for most delivery systems [96]. The pore size has been suggested to be about 60 – 200 nm, so small nanoparticles are required, and as the matrix is anionic, a cationic particle charge can also facilitate cartilage penetration [96]. So far, effective cartilage penetration has been demonstrated for polypeptide complexes [107], PAA-coated PLGA particles [57], pNIPAM-based particles [170], and PEGylated PAMAM dendrimers [190]. The conjugation of peptide targeting groups was also shown to facilitate the accumulation of delivery systems in cartilage [57, 132, 181]. Differences in penetration between OA diseased cartilage and healthy cartilage were also observed [57]. On the other hand, while small nanosized particles more effectively penetrate cartilage than larger, micrometer-sized particles, they are also cleared more rapidly from the joint. The longest *in vivo* joint retention times have been observed for particles with diameters of at least 10 μm [142, 143, 156, 160]. These particles tend to accumulate in the synovium, from which drugs can be released and delivered to other joint tissues. For example, after their release from particles, drugs can be drawn into cartilage tissue through cycles of compression and relaxation upon joint loading, the process by which nutrients are normally delivered to cartilage and wastes are cleared. Therefore, a micrometer-sized delivery system does not preclude the delivery of drugs into cartilage. Intermediately-sized particles (>200 nm to <10 μm) are eliminated at a rate that depends on the inflammatory state, which has been attributed to changes in vascular permeability with inflammation [142].

Finally, matching the right drug with a suitable delivery system will be a critical factor in the efficacy of the drug delivery system. So far, most research on particles for IA drug delivery have involved the use of corticosteroids or NSAIDs. This approach is useful for demonstrating the safety of a new drug delivery system and its potential to provide sustained drug release in the joint. However, it is well established NSAIDs and corticosteroids do not alter OA progression [20, 25]. Many new targets are emerging for OA, leading to numerous new potential disease-modifying therapies [30]. However, demonstrating the clinical efficacy and safety of these drugs has been an ongoing challenge. It is possible that regular systemic administration or a single IA injection of a small molecule or protein therapeutic may be insufficient to achieve the desired effects in the joint without dangerous side effects. Therefore, drug delivery systems can play an important role in making these potential therapies more effective. However, it is unlikely that there will be one delivery platform that will be suitable for all drugs. For each therapeutic it will be important to select and tailor the delivery system to release the appropriate concentration of drug, over the right time frame, at a suitable location in the joint. Thus, success in the future will ultimately depend on combining the right drug with right delivery system.

Acknowledgements

Removed temporarily for anonymity.

References

[1] T. Neogi, The epidemiology and impact of pain in osteoarthritis, Osteoarthr. Cartil. 21 (2013) 1145-1153.

[2] E.R. Vina, C.K. Kwoh, Edipemiology of osteoarthritis: Literature update, Curr. Opin. Rheumatol. 30 (2018) 160-167.

[3] M. Cross, E. Smith, D. Hoy, S. Nolte, I. Ackerman, M. Fransen, L. Bridgett, S. Williams, F. Guillemin, C.L. Hill, L.L. Laslett, G. Jones, F. Cicuttini, R. Osborne, T. Vos, R. Buchbinder, A. Woolf, L. March, The global burden of hip and knee osteoarthritis: Estimates from the global burden of disease 2010 study, Ann. Rheum. Dis. 73 (2014) 1323-1330.

[4] I.J. Wallace, S. Worthington, D.T. Felson, R.D. Jurmain, K.T. Wren, H. Maijanen, R.J. Woods, D.E. Lieberman, Knee osteoarthritis has doubled in prevalence since the mid-20th century, Proc. Natl. Acad. Sci. USA 114 (2017) 9332-9336.

[5] M. Hiligsmann, C. Cooper, N. Arden, M. Boers, J.C. Branco, M. Luisa Brandi, O. Bruyère, F. Guillemin, M.C. Hochberg, D.J. Hunter, J.A. Kanis, T.K. Kvien, A. Laslop, J.P. Pelletier, D. Pinto, S. Reiter-Niesert, R. Rizzoli, L.C. Rovati, J.L. Severens, S. Silverman, Y. Tsouderos, P. Tugwell, J.Y. Reginster, Health economics in the field of osteoarthritis: An expert's consensus paper from the european society for clinical and economic aspects of osteoporosis and osteoarthritis (esceo). Semin. Arthritis Rheum. 43 (2013) 303-313.

[6] S. Glyn-Jones, A.J.R. Palmer, R. Agricola, A.J. Price, T.L. Vincent, H. Weinans, A.J. Carr, Osteoarthritis, Lancet 386 (2015) 376-387.

[7] A. Fox, A. Bedi, S.A. Rodeo, The basic science of articular cartilage: Structure, composition, and function, Sports Health 1 (2009) 461-468.

[8] D.J. Hunter, A. Guermazi, Imaging techniques in osteoarthritis, PM R 4 (2012) S68-S74.

[9] R. Lui-Bryan, R. Terkeltaub, Emerging regulators of the inflammatory process in osteoarthritis, Nat. Rev. Rheumatol. 11 (2015) 35-44.

[10] H. Madry, C.N. van Dijk, M. Mueller-Gerbl, The basic science of subchondral bone, Knee Surg. Sports Traumatol. Arthrosc. 18 (2010) 419-433.

[11] T.J. Lyons, S.F. McClure, R.W. Stoddart, J. McClure, The normal human chondro-osseous junctional region: Evidence for contact of uncalcified cartilage with subchondral bone and marrow spaces, BMC Musculoskelet. Disord. 7 (2006) 52.

[12] M. Kapoor, J. Martel-Pelletier, D. Lajeunesse, J.P. Pelletier, H. Fahmi, Role of proinflammatory cytokines in the pathophysiology of osteoarthritis, Nat. Rev. Rheumatol. 7 (2011) 33-42.

[13] H. Weinans, M. Siebelt, R. Agricola, S.M. Botter, T.M. Piscaer, J.H. Waarsing, Pathophysiology of peri-articular bone changes in osteoarthritis, Bone 51 (2012) 190-196.

[14] M.D. Smith, The normal synovium, Open Rheumatol. J. 5 (2011) 100-106.

[15] J. Sellam, F. Berenbaum, The role of synovitis in pathophysiology and clinical symptoms of osteoarthritis, Nat. Rev. Rheumatol. 6 (2010) 625-635.

[16] A.Y. Hui, W.J. McCarty, K. Masuda, G.S. Firestein, R.L. Sah, A systems biology approach to synovial joint lubrication in health, injury, and disease, Wiley Interdiscip. Rev. Syst. Biol. Med. 4 (2012) 15-37.

[17] S.L. Kolasinski, T. Neogi, M.C. Hochberg, C. O'atis, G. Guyatt, J. Block, L. Callahan, C. Copenhaver, C. Dodge, D.T. Felson, K. Gellar, W.F. Harvey, G. Hawker, E. Herzig, C.K. Kwoh, A.E. Nelson, J. Samuels, C.R. Scanzello, W. White, B. Wise, R.D. Altman, D. DiRenzo, J. Fotanarosa, G. Giradi, M. Ishimori, D. Misra, A.A. Shah, A.K. Shmagel, L.M. Thoma, M. Turgenbaev, A.S. Turner, J. Reston, 2019 American College of Rheumatology/Arthritis Foundation guideline for the management of osteoarthritis of the hand, hip, and knee, Arthritis Rheumatol. 72 (2020) 220-233.

[18] P.A. Semanik, R.W. Chang, D.D. Dunlop, Aerobic activity in prevention and symptom control of osteoarthritis, PM R 4 (2012) S37-S44.

[19] M.J. Lespasio, A.A. Sultan, N.S. Piuzzi, M.E. Husni, G.F. Muschler, M.A. Mont, Hip osteoarthritis: A primer, Perm. J. 22 (2018) 17.

[20] D.S. Cheng, C.J. Visco, Pharmaceutical therapy for osteoarthritis, PM R 4 (2012) S82-S88.

[21] D. Vrdoljak, M. Selimovic, A. Marin, A. Utrobicic, P. Tugwell, L. Puljak, L. Puljak, Celecoxib for osteoarthritis, Cochrane Database Syst. Rev. 2012 (2012), CD009865.

[22] S. Haroutiunian, D.A. Drennan, A.G. Lipman, Topical NSAID therapy for musculoskeletal pain, Pain Medicine 11 (2010) 535-549.

[23] L. Mason, R.A. Moore, S. Derry, J.E. Edwards, H.J. McQuay, Systemic review of topical capsaicin for the treatment of chronic pain, BMJ 329 (2004) 991.

[24] G.S. Habib, W. Saliba, M. Nashashibi, Local effects of intra-articular steroids, Clin. Rheumatol. 29 (2010) 347-356.

[25] R.J. Douglas, Corticosteroid injection into the osteoarthritic knee: Drug selection, dose, and injection frequency, Int. J. Clin. Pract. 66 (2012) 699-704.

[26] T.E. McAlindon, M.P. LaValley, W.F. Harvey, L.L. Price, J.B. Driban, M. Zhang, R.J. Ward, Effect of intra-articular triamcinolone vs saline on knee cartilage volume and pain in patients with knee osteoarthritis: A randomized clinical trial, JAMA 317 (2017) 1967-1975.

[27] C. Zeng, N.E. Lane, D.J. Hunter, J. Wei, H.K. Choi, T.E. McAlindon, H. Li, N. Lu, G. Lei, Y. Zhang, Intra-articular corticosteroids and the risk of knee osteoarthritis progression: Results from the osteoarthritis initiative, Osteoarthr. Cartil. 27 (2019) 855-862.

[28] N. Bellamy, J. Campbell, V. Robinson, T. Gee, R. Bourne, G. Wells, Viscosupplementation for the treatment of osteoarthritis of the knee, Cochrane Database Syst. Rev. 2005 (2005) CD005321.

[29] C.W. Grayson, R.C. Decker, Total joint arthroplasty for persons with osteoarthritis, PM R 4 (2012) S97-S103.

[30] A. Latourte, M. Kloppenburg, P. Richette, Emerging pharmaceutical therapies for osteoarthritis, Nat. Rev. Rheumatol. 16 (2020) 673-688.

[31] P. Krzeski, C. Buckland-Wright, G. Bálint, G.A. Cline, K. Stoner, R. Lyon, J. Beary, W.S. Aronstein, T.D. Spector, Development of musculoskeletal toxicity without clear benefit after administration of PG-116800, a matrix metalloproteinase inhibitor, to patients with knee osteoarthritis: A randomized, 12-month, double-blind, placebo-controlled study, Arthritis Res. Ther. 9 (2007) R109.

[32] E.M. van der Aar, J. Desrivot, L. Fagard, D. Amantini, S. Larsson, A. Struglics, S. Lohmander, F. Vanhoutte, S. Dupont, ADAMTS-5 inhibitor GLPG1972, a potential new treatment in osteoarthritis, shows favorable safety, pharmacokinetics and pharmacodynamics in healthy subjects, Osteoarthr. Cartil. 26 (2018) S310.

[33] E. vanderAar, H. Deckx, M. Van Der Stoep, M. Wooning, K. Bernard, S. Grankov, O. Imbert, M. Pueyo, F. Eckstein, Study design of a phase 2 clinical trial with a disease-modifying osteoarthritis drug candidate GLPG1972/S201086: The rocella trial, Osteoarthr. Cartil. 28 (2020) S499-S500.

[34] A. Siebuhr, A.-C. Bay-Jensen, C.T. Thudium, M.A. Karsdal, B. Serruys, D. Werkmann, M. Michaelis, C. Labdel, S. Lindermann, The anti-ADAMTS-5 nanobody®, M6495, protects against cartilage breakdown in cartilage and synovial joint tissue explant models, Osteoarthr. Cartil. 26 (2018) S187.

[35] M.C. Hochberg, A. Guermazi, H. Guehring, A. Aydemir, S. Wax, P. Fleuranceau-Morel, A. Reinstrup Bihlet, I. Byrjalsen, J.R. Andersen, F. Eckstein, Effect of intra-articular sprifermin vs placebo on femorotibial joint cartilage thickness in patients with osteoarthritis the forward randomized clinical trial, JAMA 322 (2019) 1360-1370.

[36] B. Lee, J. Parvizi, D. Bramlet, D.W. Romness, A. Guermazi, M. Noh, N. Sodhi, A. Khlopas, M.A. Mont, Results of a phase ii study to determine the efficacy and safety of genetically engineered allogeneic human chondrocytes expressing TGF-β1, J. Knee Surg. 33 (2020) 167-172.

[37] P.G. Conaghan, M.A. Bowes, S.R. Kingsbury, A. Brett, G. Guillard, B. Rizoska, N. Sjögren, P. Graham, A. Jansson, C. Wadell, R. Bethell, J. Öhd, Disease-modifying effects of a novel cathepsin K inhibitor in osteoarthritis, Ann. Internal Med. 172 (2020) 86-95.

[38] R.F. Loeser, S.R. Goldring, C.R. Scanzello, M.B. Goldring, Osteoarthritis: A disease of the joint as an organ, Arthritis Rheumatol. 64 (2012) 1697-1707.

[39] C. Scoville, J. Dickson, Open-label use of anakinra (kineret) in the treatment of patients with osteoarthritis, Ind. J. Rheumatol. 12 (2017) 17-22.

[40] M. Kloppenburg, R. Ramonda, K. Bobacz, W.-Y. Kwok, D. Elewaut, T.W.J. Huizinga, F.P.B. Kroon, L. Punzi, J.S. Smolen, B. Vander Cruyssen, R. Wolterbeek, G. Verbruggen, R. Wittoek, Etanercept in patients with inflammatory hand osteoarthritis (EHOA): A multicentre, randomised, double-blind, placebo-controlled trial, Ann. Rheum. Dis. 77 (2018) 1757-1764.

[41] K. Grothe, K. Flechsenhar, T. Paehler, O. Ritzeler, J. Beninga, J. Saas, M. Herrmann, K. Rudolphi, IkappaB kinase inhibition as a potential treatment of osteoarthritis - results of a clinical proof-of-concept study, Osteoarthr. Cartil. 25 (2017) 46-52.

[42] J. Pradal, M.-F. Zuluaga, P. Maudens, J.-M. Waldburger, C.A. Seemayer, E. Doelker, C. Gabay, O. Jordan, E. Allémann, Intra-articular bioactivity of a p38 MAPK inhibitor and development of an extended-release system, Eur. J. Pharm. Biopharm. 93 (2015) 110-117.

[43] A. Ratneswaran, E.A. LeBlanc, E. Walser, I. Welch, J.S. Mort, N. Borradaile, F. Beier, Peroxisome proliferator–activated receptor promotes the progression of posttraumatic osteoarthritis in a mouse model, Arthritis Rheumatol. 67 (2015) 454-464.

[44] R. Stevens, P. Hanson, N. Wei, R. Allen, K. Guedes, R. Burges, J. Campbell, Safety and tolerability of CNTX-4975 in subjects with chronic, moderate to severe knee pain associated with osteoarthritis (OA): A pilot study, J. Pain 18 (2017) 122-129.

[45] J. Szolcsányi, Z. Sándor, Multisteric TRPV1 nocisensor: A target for analgesics, Trends Pharmacol. Sci. 33 (2012) P646-655.

[46] M.C. Hochberg, Serious joint-related adverse events in randomized controlled trials of anti-nerve growth factor monoclonal antibodies, Osteoarthr. Cartil. 23 (2015) S18-S21.

[47] C. Nguyen, F. Rannou, The safety of intra-articular injections for the treatment of knee osteoarthritis: A critical narrative review, Expert Opin. Drug Saf. 16 (2017) 897-902.

[48] C. Larsen, J. Østergaard, S.W. Larsen, H. Jensen, S. Jacobsen, C. Lindegaard, P.H. Andersen, Intra-articular depot formulation principles: Role in the management of postoperative pain and arthritic disorders, J. Pharm. Sci. 97 (2008) 4622-4654.

[49] M.A. Malone, N. Kaushik, A. Waheed, Intra-articular steroids: How soon and how often after the first injection?, SM J Community Med 2 (2016) 1014.

[50] M.B. Stephens, A.I. Beutler, F.G. O'Connor, Musculoskeletal injections: A review of the evidence, Am. Family Phys. 78 (2008) 970-976.

[51] G. Shan-Bin, T. Yue, J. Ling-Yan, Long-term sustained-released in situ gels of a water-insoluble drug amphotericin B for mycotic arthritis intra-articular administration: Preparation, in vitro and in vivo evaluation., Drug Dev. Ind. Pharm. 41 (2015) 573-582.

[52] H. Betre, W. Liu, M.R. Zalutsky, A. Chilkoti, V.B. Kraus, L.A. Setton, A thermally responsive biopolymer for intra-articular drug delivery, J. Control. Release 115 (2006) 175-182.

[53] A. Petit, M. Sandker, B. Müller, R. Meyboom, P. van Midwoud, P. Bruin, E.M. Redout, M. Versluijs-Helder, C.H.A. van der Lest, S.J. Buwalda, L.G.J. de Leede, T. Vermonden, R.J. Kok, H. Weinans, W.E. Hennink, Release behavior and intra-articular biocompatibility of celecoxib-loaded acetyl-capped PCLA-PEG-PCLA thermogels, Biomaterials 35 (2014) 7919-7928.

[54] A. Petit, E.M. Redout, C.H. van de Lest, J.C. de Grauw, B. Muller, R. Meyboom, P. van Midwoud, T. Vermonden, W.E. Hennink, P. Rene van Weeren, Sustained intra-articular release of celecoxib from in situ forming gels made of acetyl-capped PCLA-PEG-PCLA triblock copolymers in horses, Biomaterials 53 (2015) 426-36.

[55] J. Dong, D. Jiang, Z. Wang, G. Wu, L. Liao, L. Huang, Intra-articular delivery of liposomal celecoxib–hyaluronate combination for the treatment of osteoarthritis in rabbit model, Int. J. Pharm. 441 (2013) 285-290.

[56] P. Maudens, O. Jordan, E. Allémann, Recent advances in intra-articular drug delivery systems for osteoarthritis therapy, Drug Discov. Today, 23 (2018) 1761-1775.

[57] S. Brown, S. Kumar, B. Sharma, Intra-articular targeting of nanomaterials for the treatment of osteoarthritis, Acta Biomater. 93 (2019) 239-257.

[58] T.E. Kavanaugh, T.A. Werfel, H. Cho, K.A. Hasty, C.L. Duvall, Particle-based technologies for osteoarthritis detection and therapy, Drug Delivery and Translational Research, Springer Verlag, 2016, pp. 132-147.

[59] P. Chinnagounder Periyasamy, J.C.H. Leijten, P.J. Dijkstra, M. Karperien, J.N. Post, Nanomaterials for the local and targeted delivery of osteoarthritis drugs, J. Nanomater. 2012 (2012) 673968.

[60] M.L. Kang, G.I. Im, Drug delivery systems for intra-articular treatment of osteoarthritis, Expert Opin. Drug Delivery, 11 (2014) 269-282.

[61] M. Rahimi, G. Charmi, K. Matyjaszewski, X. Banquy, J. Pietrasik, Recent developments in natural and synthetic polymeric drug delivery systems used for the treatment of osteoarthritis, Acta Biomater. https://doi.org/10.1016/j.actbio.2021.01.003 (2021).

[62] V. Irawan, T.-C. Sung, A. Higuchi, T. Ikoma, Collagen scaffolds in cartilage tissue engineering and relevant approaches for future development, Tissue Eng. Regen. Med. 15 (2018) 673-697.

[63] S.A. Ahsan, M. Thomas, K.K. Reddy, S. Gopal Sooraparaju, A. Asthana, I. Bhatnagar, Chitosan as biomaterial in drug delivery and tissue engineering, Int. J. Biol. Macromol. 110 (2018) 97-109.

[64] H. Knopf-Marques, M. Pravada, L. Wolfova, V. Velebny, P. Schaaf, N. Engin Vrana, P. Lavalle, Hyaluronic acid and its derivatives in coating and delivery systems: Applications in tissue engineering, regenerative medicine and immunomodulation, Adv. Healthcare Mater. 5 (2016) 2841-2855.

[65] D. Melani Hariyadi, N. Islam, Current status of alginate in drug delivery, Adv. Pharmcol. Pharmaceut. Sci. 2020 (2020) 8886095.

[66] S.-B. Park, E. Lih, E.-S. Park, Y.K. Joung, D.K. Han, Biopolymer-based functional composites for medical applications, Prog. Polym. Sci. 68 (2017) 77-105.

[67] A. Bernkop-Schnürch, S. Dünnhaupt, Chitosan-based drug delivery systems, Eur. J. Pharm. Biopharm. 81 (2012) 463-469.

[68] L. Hu, Y. Sun, Y. Wu, Advances in chitosan-based drug delivery vehicles, Nanoscale 5 (2013) 3103-3111.

[69] A. Moeini, P. Pedram, P. Makvandi, M. Malinconico, G. Gomez d'Ayala, Wound healing and antimicrobial effect of active secondary metabolites in chitosan-based wound dressings: A review, Carbohydrate Polym. 233 (2020) 115839.

[70] H. Abd-Allah, A.O. Kamel, O.A. Sammour, Injectable long acting chitosan/tripolyphosphate microspheres for the intra-articular delivery of lornoxicam: Optimization and in vivo evaluation, Carbohydrate Polym. 149 (2016) 263-273.

[71] P. Chen, C. Xia, S. Mei, J. Wang, Z. Shan, X. Lin, S. Fan, Intra-articular delivery of sinomenium encapsulated by chitosan microspheres and photo-crosslinked GelMA hydrogel ameliorates osteoarthritis by effectively regulating autophagy, Biomaterials 81 (2016) 1-13.

[72] Y. Sun, Y. Yao, C.Z. Ding, A combination of sinomenine and methotrexate reduces joint damage of collagen induced arthritis in rats by modulating osteoclast-related cytokines, Int. Immunopharmacol. 18 (2014) 135-141.

[73] Y.-R. Zhou, Y. Zhao, B.-H. Bao, J.-X. Li, Snd-117, a sinomenine bivalent alleviates type II collagen-induced arthritis in mice, Int. Immunopharmacol. 26 (2015) 423-431.

[74] M.L. Kang, J.Y. Ko, J.E. Kim, G.I. Im, Intra-articular delivery of kartogenin-conjugated chitosan nano/microparticles for cartilage regeneration, Biomaterials, 35 (2014) 9984-9994.

[75] K. Johnson, S. Zhu, M.S. Tremblay, J.N. Payette, J. Wang, L.C. Bouchez, S. Meeusen, A. Althage, C.Y. Cho, X. Wu, P.G. Schultz, A stem cell-based approach to cartilage repair, Science 336 (2012) 717-721.

[76] Y. Ono, S. Ishizuka, C.B. Knudson, W. Knudson, Chondroprotective effect of kartogenin on CD44-mediated functions in articular cartilage and chondrocytes, Cartilage 5 (2014) 172-180.

[77] M.L. Kang, J.E. Kim, G.I. Im, Thermoresponsive nanospheres with independent dual drug release profiles for the treatment of osteoarthritis, Acta Biomater. 39 (2016) 65-78.

[78] Y. Zhou, S.-Q. Liu, H. Peng, L. Yu, B. He, Q. Zhao, In vivo anti-apoptosis activity of novel berberine-loaded chitosan nanoparticles effectively ameliorates osteoarthritis, Int. Immunopharmacol. 28 (2015) 34-43.

[79] H. Zhao, T. Zhang, C. Xia, L. Shi, S. Wang, X. Zheng, T. Hu, B. Zhang, Berberine ameliorates cartilage degeneration in interleukin-1β-stimulated rat chondrocytes and in a rat model of osteoarthritis via AKT signalling, J. Cellular. Mol. Med. 18 (2014) 283-292.

[80] E. Russo, N. Gaglianone, S. Baldassari, B. Parodi, I. Croce, A.M. Bassi, S. Vernazza, G. Caviglioli, Chitosan-clodronate nanoparticles loaded in poloxamer gel for intra-articular administration, Colloids Surf., B 143 (2016) 88-96.

[81] N. Makkonen, A. Saliminen, M.J. Rogers, J.C. Frith, A. Urtti, E. Azhayeva, J. Mönkkönen, Contrasting effects of alendronate and clodronate on raw 264 macrophages: The role of a bisphosphonate metabolite, Eur. J. Pharm. Sci. 8 (1999) 109-118.

[82] M. Muratore, E. Quarta, F. Calcagnile, L. Quarta, Clinical utility of clodronate in the prevention and management of osteoporosis in patients intolerant of oral bisphosphonates, Drug Des. Devel. Ther. 2011 (2011) 445-454.

[83] H.-J. Li, X.-F. Xu, M. Gong, B. Qiu, Chitosan-p CrmA nanoparticles protect against cartilage degradation of osteoarthritis in a rabbit model, Int. J. Clin. Exp. Med. 11 (2018) 11619-11630.

[84] B.L. Ma, P.H. Zhou, T. Xie, L. Shi, B. Qiu, Q. Wang, Inhibition of interleukin-1beta-stimulated dedifferentiation of chondrocytes via controlled release of CrmA from hyaluronic acid-chitosan microspheres, BMC Musculoskelet. Disord. 16 (2015) 61.

[85] J. Dobo, R. Swanson, G.S. Salvesen, S.T. Olsen, P.G. Gettins, Cytokine response modifier a inhibition of initiator caspases results in covalent complex formation and dissociation of the caspase tetramer, J. Biol. Chem. 281 (2006) 38781-38790.

[86] R.D. Altman, A. Manjoo, A. Fierlinger, F. Niazi, M. Micholls, The mechanism of action for hyaluronic acid treatment in the osteoarthritis knee: A systematic review, BMC Musculoskelet. Disord. 16 (2015) 321.

[87] Ş. Şahin, E. Bilgiç, K. Salimi, A. Tuncel, B. Karaosmanoğlu, E.Z. Taşkıran, P. Korkusuz, F. Korkusuz, Development, characterization and research of efficacy on in vitro cell culture of glucosamine carrying hyaluronic acid nanoparticles, J. Drug Deliv. Sci. Technol., 52 (2019) 393-402.

[88] T. Pham, A. Cornea, K.E. Blick, A. Jenkins, R.H. Scofield, Oral glucosamine in doses used to treat osteoarthritis worsens insulin resistance, Am. J. Med. Sci. 333 (2007) 333-339.

[89] S. Persiani, R. Rotini, G. Trisolino, L.C. Rovati, M. Locatelli, D. Paganini, D. Antonioli, A. Roda, Synovial and plasma glucosamine concentrations in osteoarthritic patients following oral crystalline glucosamine sulphate at therapeutic dose, Osteoarthr. Cartil. 15 (2007) 764-772.

[90] R. El-Gogary, M.A. Khattab, H. Abd-Allah, Intra-articular multifunctional celecoxib loaded hyaluronan nanocapsules for the suppression of inflammation in an osteoarthritic rat model, Int. J. Pharm. 583 (2020) 119378.

[91] J. Wang, X. Wang, Y. Cao, T. Huang, D.-X. Song, H.-R. Tao, Therapeutic potential of hyaluronic acid/chitosan nanoparticles for the delivery of curcuminoid in knee osteoarthritis and an in vitro evaluation in chondrocytes, Int. J. Mol. Med. 42 (2018) 2604-2614.

[92] X. Li, K. Feng, J. Li, D. Yu, Q. Fan, T. Tang, X. Yao, X. Wang, Curcumin inhibits apoptosis of chondrocytes through activation erk1/2 signaling pathways induced autophagy, Nutrients 9 (2017) E414.

[93] R.-H. Deng, B. Qiu, P.H. Zhou, Chitosan/hyaluronic acid/plasmid-DNA nanoparticles encoding interleukin-1 receptor antagonist attenuate inflammation in synoviocytes induced by interleukin-1 beta, J. Mater. Sci.: Mater. Med. 29 (2018) 155.

[94] R.L. Smeets, F.A. van de Loo, L.A. Joosten, O.J. Arntz, M.B. Bennink, W.A. Loesberg, I.P. Dmitriev, D.T. Curiel, M.U. Martin, W.B. van den Berg, Effectiveness of the soluble form of the interleukin-1 receptor accessory protein as an inhibitor of interleukin-1 in collagen-induced arthritis, Arthritis Rheumatol. 48 (2003) 2949-2958.

[95] B. Qiu, X.-F. Xu, R.-H. Deng, G.-Q. Xia, X.-F. Shang, P.H. Zhou, Hyaluronic acid-chitosan nanoparticles encoding crma attenuate interleukin-1β induced inflammation in synoviocytes in vitro, Int. J. Mol. Med. 43 (2019) 1076-1084.

[96] A.G. Bajpayee, A.J. Grodzinsky, Cartilage-targeting drug delivery: Can electrostatic interactions help?, Nat. Rev. Rheumatol. 13 (2017) 183-193.

[97] J.A. Singh, S. Noorbaloochi, R. MacDonald, L.J. Maxwell, Chondroitin for osteoarthritis, Cochrane Database Syst. Rev. 2015 (2015) CD005614.

[98] T.-N. Tsai, H.-J. Yen, C.-C. Chen, Y.-C. Chen, Y.-A. Young, K.-M. Cheng, J.-J. Young, P.-D. Hong, Novel protein-loaded chondroitin sulfate-n-[(2-hydroxy-3-trimethylammonium)propyl]chitosan nanoparticles with reverse zeta potential: Preparation, characterization, and ex vivo assessment, J. Mater. Chem. B 3 (2015) 8729-8737.

[99] D. Ramdhani, Formulation and characterization of chondroitin sulfate nanoparticle with chitosan as polymer and kappa carrageenan as crosslinker using the ionic gelation method, J. Nanomed. Nanotechnol. S8 (2017) 005.

[100] S.R. MacEwan, A. Chilkoti, Applications of elastin-like polypeptides in drug delivery, J. Control. Release 190 (2014) 314-330.

[101] H. Sun, X. Gu, Q. Zhang, H. Xu, Z. Zhong, C. Deng, Cancer nanomedicines based on synthetic polypeptides, Biomacromolecules 20 (2019) 4299-4311.

[102] T.K. Mwangi, R.D. Bowles, D.M. Tainter, R.D. Bell, D.L. Kaplan, L.A. Setton, Synthesis and characterization of silk fibroin microparticles for intra-articular drug delivery, Int. J. Pharm. 485 (2015) 7-14.

[103] K. Numata, D.L. Kaplan, Silk-based delivery systems of bioactive molecules, Adv. Drug Delivery Rev. 62 (2010) 1497-1508.

[104] Y. Cao, B. Wang, Biodegradation of silk biomaterials, Int. J. Mol. Sci. 10 (2009) 1514-1524.

[105] L. Meinel, S. Hofmann, V. Karageorgiou, C. Kirker-Head, J. McCool, G. Gronowicz, L. Zichner, R. Langer, G. Vunjak-Novakovic, D.L. Kaplan, The inflammatory responses to silk films in vitro and in vivo, Biomaterials 26 (2005) 147-155.

[106] B. Crivelli, E. Bari, S. Perteghella, L. Catenacci, M. Sorrenti, M. Mocchi, S. Faragò, G. Tripodo, A. Prina-Mello, M.L. Torre, Silk fibroin nanoparticles for celecoxib and curcumin delivery: ROS-scavenging and anti-inflammatory activities in an in vitro model of osteoarthritis, Eur. J. Pharm. Biopharm. 137 (2019) 37-45.

[107] N.J. Shah, B.C. Geiger, M.A. Quadir, N. Hyder, Y. Krishnan, A.J. Grodzinsky, P.T. Hammond, Synthetic nanoscale electrostatic particles as growth factor carriers for cartilage repair, Bioeng. Transl. Med. 1 (2016) 347-356.

[108] M. Schmidt, E. Chen, S. Lynch, A review of the effects of insulin-like growth factor and platelet derived growth factor on in vivo cartilage healing and repair, Osteoarthr. Cartil. 14 (2006) 403-412.

[109] F. Danhier, E. Ansorenaa, J.M. Silva, R. Coco, A. Le Breton, P. V., PLGA-based nanoparticles: An overview of biomedical applications, J. Control. Release 161 (2012) 505-522.

[110] A. Pandey, D.S. Jain, S. Chakraborty, Poly lactic-co-glycolic acid (PLGA) copolymer and its pharmaceutical application, in: K.V. Thakur, M.K. Thakur (Eds.), Handbook of polymers for pharmaceutical technologies, Scrivener Publishing, Beverly, MA, 2015, pp. 151-172.

[111] J.M. Anderson, M.S. Shive, Biodegradation and biocompatibility of PLA and PLGA microspheres, Adv. Drug Delivery Rev. 28 (1997) 5-24.

[112] P.G. Conaghan, D.J. Hunter, S.B. Cohen, V.B. Kraus, F. Berenbaum, D.E. Lieberman, D.G. Jones, A.I. Spitzer, D.S. Jevsevar, N.P. Katz, D.J. Burgess, J. Lufkin, J.R. Johnson, N. Bodick, Effects of a single intra-articular injection of a microsphere formulation of triamcinolone acetonide on knee osteoarthritis pain, J. Bone Joint Surg. Am. 100 (2018) 666-77.

[113] A. Kumar, A.M. Bendele, R.C. Blanks, N. Bodick, Sustained efficacy of a single intraarticular dose of FX006 in a rat model of repeated localized knee arthritis, Osteoarthr. Cartil. 23 (2015) 151-160.

[114] V.B. Kraus, P.G. Conaghan, H.A. Aazami, P. Mehra, A.J. Kivitz, J. Lufkin, J. Hauben, J.R. Johnson, N. Bodick, Synovial and systemic pharmacokinetics (PK) of triamcinolone acetonide (TA) following intra-articular (IA) injection of an extendedrelease microsphere-based formulation (FX006) or standard crystalline suspension in patients with knee osteoarthritis (OA), Osteoarthr. Cartil. 26 (2018) 34-42.

[115] H.Y. Yang, M. Van Dijk, R. Licht, M. Beekhuizen, M. Van Rijen, M.K. Janstål, F.C. Öner, W.J.A. Dhert, D. Schumann, L.B. Creemers, Applicability of a newly developed bioassay

for determining bioactivity of anti-inflammatory compounds in release studies - celecoxib and triamcinolone acetonide released from novel PLGA-based microspheres, Pharm. Res. 32 (2015) 680-690.

[116] S.R. Kim, M.J. Ho, E. Lee, J.W. Lee, Y.W. Choi, M.J. Kang, Cationic PLGA/Eudragit RL nanoparticles for increasing retention time in synovial cavity after intra-articular injection in knee joint, Int. J. Nanomedicine 10 (2015) 5263-5271.

[117] S.R. Kim, M.J. Ho, S.H. Kim, H.R. Cho, H.S. Kim, Y.S. Choi, Y.W. Choi, M.J. Kang, Increased localized delivery of piroxicam by cationic nanoparticles after intra-articular injection, Drug Des. Devel. Ther. 10 (2016) 3779-3787.

[118] N. Goto, K. Okazaki, Y. Akasaki, K. Ishihara, K. Murakami, K. Koyano, Y. Ayukawa, N. Yasunami, T. Masuzaki, Y. Nakashima, Single intra-articular injection of fluvastatin-PLGA microspheres reduces cartilage degradation in rabbits with experimental osteoarthritis, J. Orthop. Res. 35 (2017) 2465-2475.

[119] P.D. Thompson, P. Clarkson, R.H. Karas, Statin-associated myopathy, JAMA 289 (2003) 1681-1690.

[120] C. Gómez-Gaete, M. Retamal, C. Chávez, P. Bustos, R. Godoy, P. Torres-Vergara, Development, characterization and in vitro evaluation of biodegradable rhein-loaded microparticles for treatment of osteoarthritis, Eur. J. Pharm. Sci. 44 (2017) 390-397.

[121] C. Gómez-Gaete, F. Ferreira, P. Bustos, S. Mennickent, D. Castillo, C. Chávez, P. Novoa, R. Godoy, Optimization of rhein-loaded polymeric nanoparticles using a factorial design and evaluation of the cytotoxic and anti-inflammatory effects, Drug Dev. Ind. Pharm. 96 (2018) 1285-1294.

[122] E.M. Bartels, H. Bliddal, P.K. Schøndorff, R.D. Altman, W. Zhang, R. Christensen, Symptomatic efficacy and safety of diacerein in the treatment of osteoarthritis: A meta-analysis of randomized placebo-controlled trials., Osteoarthr. Cartil. 18 (2010) 289-296.

[123] P. Nicolas, M. Tod, C. Padoin, O. Petitjean, Clinical pharmacokinetics of diacerein, Clin. Pharmacokinetics 35 (1998) 347-359.

[124] M. Farr, K. Garvey, A.M. Bold, M.J. Kendall, P.A. Bacon, Significance of the hydrogen ion concentration in synovial fluid in rheumatoid arthritis, Clin. Exp. Rheumatol. 3 (1985) 99-104.

[125] L. Zerrillo, I. Que, O. Vepris, L.N. Morgado, A. Chan, K. Bierau, Y. Li, F. Galli, E. Bos, R. Censi, P. Di Martino, G.J.V.M. van Osch, L.J. Cruz, pH-responsive poly(lactide-co-glycolide) nanoparticles containing nearinfrared dye for visualization and hyaluronic acid for treatment of osteoarthritis, J. Control. Release 309 (2019) 265-276.

[126] E. Alarçin, Ç. Demirbağ, S. Karsli-Ceppioglu, O. Kerimoğlu, A. Bal-Ozturk, Development and characterization of oxaceprol-loaded poly-lactide-co-glycolide nanoparticles for the treatment of osteoarthritis, Drug Devel. Res., 81 (2020) 501-510.

[127] G. Herrmann, D. Steeger, M. Klasser, J. Wirbitzky, M. Fürst, R. Venbrocks, H. Rohde, D. Jungmichel, H.D. Hildebrandt, M.J. Parnham, W. Gimbel, H. Dirschedl, Oxaceprol is a well-tolerated therapy for osteoarthritis with efficacy equivalent to diclofenac, Clin. Rheumatol. 19 (1999) 99-104.

[128] K. Kruger, M. Klasser, J. Mossinger, U. Becker, Oxaceprol-a randomised, placebo-controlled clinical study in osteoarthritis with a non-conventional non-steroidal anti-inflammatory drug, Clin. Exp. Rheumatol. 25 (2007) 29-34.

[129] H.J. Shin, H. Park, N. Shin, H.H. Kwon, Y. Yin, J.A. Hwang, S.I. Kim, S.R. Kim, S. Kim, Y. Joo, Y. Kim, J. Kim, J. Beom, D.W. Kim, p47phox siRNA-loaded PLGA nanoparticles suppress ROS/oxidative stress-induced chondrocyte damage in osteoarthritis, Polymers 12 (2020) 443.

[130] H.J. Shin, H. Park, N. Shin, J. Shin, D.H. Gwon, H.H. Kwon, Y. Yin, J.A. Hwang, J. Hong, J.Y. Heo, C.S. Kim, Y. Joo, Y. Kim, J. Kim, J. Beom, D.W. Kim, p66shc siRNA nanoparticles ameliorate chondrocytic mitochondrial dysfunction in osteoarthritis, Int. J. Nanomedicine 15 (2020) 2379-2390.

[131] A. Panday, M.K. Sahoo, D. Osorio, S. Batra, NADPH oxidases: An overview from structure to innate immunity-associated pathologies, Cell Mol. Immunol. 12 (2015) 5-23.

[132] S.B. Brown, L. Wang, R.R. Jungels, B. Sharma, Effects of cartilage-targeting moieties on nanoparticle biodistribution in healthy and osteoarthritic joints, Acta Biomater. 101 (2020) 469-483.

[133] K.M. Dhanabalan, V. Gupta, R. Agarwal, Rapamycin-PLGA microparticles prevent senescence, sustain cartilage matrix production under stress and exhibit prolonged retention in mouse joints, Biomater. Sci. 8 (2020) 4308-4321.

[134] B. Carames, N. Taniguchi, S. Otsuki, F.J. Blanco, M. Lotz, Autophagy is a protective mechanism in normal cartilage, and its aging-related loss is linked with cell death and osteoarthritis, Arthritis Rheum. 62 (2010) 791-801.

[135] M.V. Blagosklonny, Rapamycin, proliferation and geroconversion to senescence, Cell Cycle 17 (2018) 2655-2665.

[136] R.F. Loeser, Aging and osteoarthritis: The role of chondrocyte senescence and aging changes in the cartilage matrix, Osteoarth. Cartil. 17 (2009) 971-979.

[137] R.T. Abraham, G.J. Wiederrecht, Immunopharmacology of rapamycin, Annu. Rev. Immunol. 14 (1996) 483-510.

[138] X. Ai, Y. Duan, Q. Zhang, D. Sun, R.H. Fang, W. Gao, L. Zhang, R. Liu-Bryan, Cartilage-targeting ultrasmall lipid-polymer hybrid nanoparticles for the prevention of cartilage degradation, Bioeng. Transl. Med. 6 (2021) e10187.

[139] L.Y. Chen, Y. Wang, R. Terkeltaub, R. Liu-Bryan, Activation of AMPKSIRT3 signaling is chondroprotective by preserving mitochondrial DNA integrity and function, Osteoarthr. Cartil. 26 (2018) 1539-1550.

[140] B. Tyler, D. Gullotti, A. Mangraviti, T. Utsuki, H. Brem, Polylactic acid (PLA) controlled delivery carriers for biomedical applications, Adv. Drug Delivery Rev. 107 (2016) 163-175.

[141] A. Jain, K. Reddy Kunduru, M. Basu, A.J. Domb, W. Khan, Injectable formulations of poly(lactic acid) and its copolymers in clinical use, Adv. Drug Delivery Rev. 107 (2016) 213-227.

[142] J. Pradal, P. Maudens, C. Gabay, C.A. Seemayer, O. Jordan, E. Allémann, Effect of particle size on the biodistribution of nano- and microparticles following intra-articular injection in mice, Int. J. Pharm. 498 (2016) 119-129.

[143] P. Maudens, C.A. Seemayer, F. Pfefferlé, O. Jordan, E. Allémann, Nanocrystals of a potent p38 mapk inhibitor embedded in microparticles: Therapeutic effects in inflammatory and mechanistic murine models of osteoarthritis, J. Control. Release 276 (2018) 102-112.

[144] P. Maudens, C.A. Seemayer, C. Thauvin, C. Gabay, O. Jordan, E. Allémann, Nanocrystal–polymer particles: Extended delivery carriers for osteoarthritis treatment, Small 14 (2018) 1703108.

[145] E. Malikmammadova, T. Endogan Tanira, A. Kiziltaya, V. Hasircia, V. Hasircia, PCL and PCL-based materials in biomedical applications, J. Biomater. Sci., Polym. Ed. 29 (2018) 863-893.

[146] M.A. Woodruff, D.W. Hutmacher, The return of a forgotten polymer - polycaprolactone in the 21st century., Prog. Polym. Sci. 35 (2010) 1217-1256.

[147] R. Gutwald, H. Pistner, J. Reuther, J. Muhling, Biodegradation and tissue-reaction in a long-term implantation study of poly(l-lactide), J. Mater. Sci. Mater. Med. 5 (1994) 485-490.

[148] O. Aydin, F. Korkusuz, P. Korkusuz, A. Tezcaner, E. Bilgic, V. Yaprakci, D. Keskin, In vitro and in vivo evaluation of doxycycline-chondroitin sulfate/PCL microspheres for intraarticular treatment of osteoarthritis, J. Biomed. Mater. Res., Part B, 103 (2015) 1238-1248.

[149] T.J. Blumberg, R.M. Natoli, K.A. Athanasiou, Effects of doxycycline on articular cartilage gag release and mechanical properties following impact, Biotechnol. Bioeng. 100 (2008) 506-515.

[150] P. Arunkumara, S. Indulekhab, S. Vijayalakshmia, R. Srivastavab, Synthesis, characterizations, in vitro and in vivo evaluation of etoricoxib-loaded poly(caprolactone) microparticles – a potential intra-articular drug delivery system for the treatment of osteoarthritis, J. Biomater. Sci., Polym. Ed. 27 (2016) 303-316.

[151] A.C. Fonseca, M.H. Gil, P.N. Simoes, Biodegradable poly(ester amide)s - a remarkable opportunity for the biomedical area: Review on the synthesis, characterization and applications, Prog. Polym. Sci. 39 (2014) 1291-1311.

[152] A. Soleimani, S. Drappel, R. Carlini, A. Goredema, E.R. Gillies, Structure-property relationships for a series of poly(ester amide)s containing amino acids, Ind. Eng. Chem. Res. 53 (2014) 1452-1460.

[153] A. Díaz, R. Katsarava, J. Puiggalí, Synthesis, properties and applications of biodegradable polymers derived from diols and dicarboxylic acids: From polyesters to poly(ester amide)s, Int. J. Mol. Sci. 15 (2014) 7064-7123.

[154] D.K. Knight, E.R. Gillies, K. Mequanint, Strategies in functional poly(ester amide) syntheses to study human coronary artery smooth muscle cell interactions, Biomacromolecules 12 (2011) 2475-2487.

[155] M. Deng, J. Wu, C.A. Reinhart-King, C.C. Chu, Synthesis and characterization of biodegradable poly(ester amide)s with pendant amine functional groups and in vitro cellular response., Biomacromolecules 10 (2009) 3037-3047.

[156] M. Janssen, U.T. Timur, N. Woike, T.J.M. Welting, G. Draaisma, M. Gijbels, L.W. van Rhijn, G. Mihov, J. Thies, P.J. Emans, Celecoxib-loaded PEA micropheres as an auto regulatory drug-delivery system after intra-articular injection, J. Control. Release 244 (2016) 30-40.

[157] R. Sharony, P.-J. Yu, J. Park, A.C. Galloway, P. Mignatti, G. Pintucci, Protein targets of inflammatory serine proteases and cardiovascular disease, J. Inflammation 7 (2010) Article number: 45.

[158] S. Nakano, T. Ikata, I. Kinoshita, J. Kanematsu, S. Yasuoka, Characteristics of the protease activity in synovial fluid from patients with rheumatoid arthritis and osteoarthritis, Clin. Exp. Rheumatol. 17 (1999) 161-170.

[159] S.O. Carrigan, A.L. Weppler, A.C. Issekutz, A.W. Stadnyk, Neutrophil differentiated HL-60 cells model Mac-1 (CD11b/CD18)-independent neutrophil transepithelial migration, Immonology 115 (2005) 108-117.

[160] I. Rudnik-Jansen, S. Colen, J. Berard, S. Plomp, I. Que, M. van Rijen, N. Woike, A. Egas, G. van Osch, E. van Maarseveen, K. Messier, A. Chan, J. Thies, L. Creemers, Prolonged inhibition of inflammation in osteoarthritis by triamcinolone acetonide released from a polyester amide microsphere platform, J Control. Release 253 (2017) 64-72.

[161] I.J. Villamagna, T.N. Gordon, M.B. Hurtig, F. Beier, E.R. Gillies, Poly(ester amide) particles for controlled delivery of celecoxib, J. Biomed. Mater. Res., Part A 107 (2019) 1235-1243.

[162] I.J. Villamagna, D.M. McRae, A. Borecki, X. Mei, F. Lagugné-Labarthet, F. Beier, E.R. Gillies, GSK3787-loaded poly(ester amide) particles for intra-articular drug delivery, Polymers 12 (2020) 736.

[163] A. Bordat, T. Boissenot, J. Nicolas, N. Tsapis, Thermoresponsive polymer nanocarriers for biomedical applications, Adv. Drug Delivery Rev. 138 (2019) 167–192.

[164] K. Nagase, M. Yamato, H. Kanazawa, T. Okano, Poly(n-isopropylacrylamide)-based thermoresponsive surfaces provide new types of biomedical applications, Biomaterials 153 (2018) 27-48.

[165] M. Rey, M.A. Fernandez-Rodriguez, M. Karg, L. Isa, N. Vogel, Poly-n-isopropylacrylamide nanogels and microgels at fluid interfaces, Acc. Chem. Res. 53 (2020) 414-424.

[166] S. Poh, J.B. Lin, A. Panitch, Release of anti-inflammatory peptides from thermosensitive nanoparticles with degradable cross-links suppresses pro-inflammatory cytokine production, Biomacromolecules 16 (2015) 1191-1200.

[167] P. Maudens, S. Meyer, C.A. Seemayer, O. Jordan, E. Allémann, Self-assembled thermoresponsive nanostructures of hyaluronic acid conjugates for osteoarthritis therapy, Nanoscale 10 (2018) 1845-1854.

[168] R.L. Bartlett II, S. Sharma, A. Panitch, Cell-penetrating peptides released from thermosensitive nanoparticles suppress pro-inflammatory cytokine response by specifically targeting inflamed cartilage explants, Nanomedicine: Nanotechnol. Biol. Med. 9 (2013) 419-427.

[169] J.B. Lin, S. Poh, A. Panitch, Controlled release of anti-inflammatory peptides from reducible thermosensitive nanoparticles suppresses cartilage inflammation, Nanomedicine: Nanotechnol. Biol. Med. 12 (2016) 2095-2100.

[170] J. McMasters, S. Poh, J.B. Lin, A. Panitch, Delivery of anti-inflammatory peptides from hollow PEGylated poly(NIPAM) nanoparticles reduces inflammation in an ex vivo osteoarthritis model, J. Control. Release 258 (2017) 161-170.

[171] M. Deloney, K. Smart, B.A. Christiansen, A. Panitch, Thermoresponsive, hollow, degradable core-shell nanoparticles for intra-articular delivery of anti-inflammatory peptide, J. Control. Release 323 (2020) 47-58.

[172] J.L. Brugnano, B.K. Chan, B.L. Seal, A. Panitch, Cell-penetrating peptides can confer biological function: Regulation of inflammatory cytokines in human monocytes by MK2 inhibitor peptides, J. Control. Release 155 (2011) 128-133.

[173] K. Zhang, J. Yang, Y. Sun, M. He, J. Liang, J. Luo, W. Cui, L. Deng, X. Xu, B. Wang, H. Zhang, Thermo-sensitive dual-functional nanospheres with enhanced lubrication and drug delivery for the treatment of osteoarthritis, Chem. Eur. J. 26 (2020) 10564-10574.

[174] H. Chen, T. Sun, Y. Yan, X. Jia, Y. Sun, X. Zhao, J. Qi, W. Cui, L. Deng, H. Zhang, Cartilage matrix-inspired biomimetic superlubricated nanospheres for treatment of osteoarthritis, Biomaterials 242 (2020) 119931.

[175] L. Yang, Y. Liu, X. Shou, D. Ni, T. Kong, Y. Zhao, Bio-inspired lubricant drug delivery particles for the treatment of osteoarthritis, Nanoscale 12 (2020) 17093-17102.

[176] A. Getgood, A. Dhollander, A. Malone, J. Price, J. Helliwell, Pharmacokinetic profile of intra-articular fluticasone propionate microparticles in beagle dog knees, Cartilage 10 (2019) 139-147.

[177] T.H. Epps III, R.K. O'Reilly, Block copolymers: Controlling nanostructure to generate functional materials – synthesis, characterization, and engineering, Chem. Sci. 7 (2016) 1674-1689.

[178] N.J.W. Penfold, J. Yeow, C. Boyer, S.P. Armes, Emerging trends in polymerization-induced self-assembly, ACS Macro Lett. 8 (2019) 1029-1054.

[179] A. Singh, R. Agarwal, C.A. Diaz-Ruiz, N.J. Willett, P. Wang, L.A. Lee, Q. Wang, R.E. Guldberg, A.J. García, Nanoengineered particles for enhanced intra-articular retention and delivery of proteins, Adv. Healthcare Mater. 3 (2014) 1562-1567.

[180] R. Agarwal, T.M. Volkmer, P. Wang, L.A. Lee, Q. Wang, A.J. García, Synthesis of self-assembled IL-1Ra-presenting nanoparticles for the treatment of osteoarthritis, J. Biomed. Mater. Res., Part A 104 (2015) 595-599.

[181] T. Jiang, H.-M. Kan, K. Rajpura, E.J. Carbone, Y. Li, K.W.-H. Lo, Development of targeted nanoscale drug delivery system for osteoarthritis cartilage tissue, J. Nanosci. Nanotechnol. 18 (2018) 2310-2317.

[182] W. Fan, J. Li, L. Yuan, J. Chen, Z. Wang, Y. Wang, C. Guo, X. Mo, Z. Yan, Intra-articular injection of kartogenin-conjugated polyurethane nanoparticles attenuates the progression of osteoarthritis, Drug Delivery 25 (2018) 1004-1012.

[183] X. Liu, C. Corciulo, S. Arabagian, A. Ulman, B.N. Cronstein, Adenosine-functionalized biodegradable PLA-b-PEG nanoparticles ameliorate osteoarthritis in rats, Sci. Rep. 9 (2019) 7430.

[184] Y. Wei, L. Luo, T. Gui, F. Yu, L. Yan, L. Yao, L. Zhong, W. Yu, B. Han, J.M. Patel, J.F. Liu, F. Beier, L.S. Levin, C. Nelson, Z. Shao, L. Han, R.L. Mauck, A. Tsourkas, J. Ahn, Z. Cheng, L. Qin, Targeting cartilage EGFR pathway for osteoarthritis treatment, Sci. Transl. Med. 13 (2021) eabb3946.

[185] L. Qin, F. Beier, EGFR signaling: Friend or foe for cartilage?, JBMR Plu 3 (2019) e10177.

[186] Designing Dendrimers, S. Campagna, P. Ceroni, F. Puntoriero Eds.; John Wiley and Sons, Inc., Hoboken, 2012.

[187] E.R. Gillies, J.M.J. Fréchet, Dendrimers and dendritic polymers in drug delivery, Drug Discov.Today 10 (2005) 35-43.

[188] H. Wang, Q. Huang, H. Chang, J. Xiao, Y. Cheng, Stimuli-responsive dendrimers in drug delivery, Biomater. Sci. 4 (2016) 375-390.

[189] Q. Hu, B. Ding, X. Yan, L. Peng, J. Duan, S. Yang, L. Cheng, D. Chen, Polyethylene glycol modified pamam dendrimer delivery of kartogenin to induce chondrogenic differentiation of mesenchymal stem cells, Nanomedicine: Nanotechnol. Biol. Med. 13 (2017) 2189-2198.

[190] B.C. Geiger, S. Wang, R.F. Padera, A.J. Grodzinsky, P.T. Hammond, Cartilage-penetrating nanocarriers improve delivery and efficacy of growth factor treatment of osteoarthritis, Sci. Transl. Med., 2018, p. eaat8800.

[191] S. Biswas, P. Kumari, P.M. Lakhani, B. Ghosh, Recent advances in polymeric micelles for anti-cancer drug delivery, Eur. J. Pharm. Sci. 83 (2016) 184-202.

[192] M. Shahriari, M. Zahiri, K. Adbnous, S.M. Taghdisi, M. Ramezani, M. Alibolandi, Enzyme responsive drug delivery systems in cancer treatment, J. Control. Release 308 (2019) 172-189.

[193] E.R. Gillies, Reflections on the evolution of smart polymers, Israel J. Chem. 60 (2020) 75-85.

[194] T. Kean, M. Thanou, Biodegradation, biodistribution and toxicity of chitosan, Adv. Drug Delivery Rev. 62 (2010) 3-11.

[195] J. Patterson, R. Siew, S.W. Herring, A.S.P. Lin, R. Guldberg, P.S. Stayton, Hyaluronic acid hydrogels with controlled degradation properties for oriented bone regeneration, Biomaterials 31 (2010) 6772-6781.

[196] R. Benito-Arenas, S.G. Zárate, J. Revuelta, A. Bastida, Chondroitin sulfate-degrading enzymes as tools for the development of new pharmaceuticals, Catalysts 9 (2019) 322.

[197] J. Rosales-Alexander, J. Balsalobre Aznar, C. Magro-Checa, Calcium pyrophosphate crystal deposition disease: Diagnosis and treatment, Open Access Rheumatol. 6 (2014) 39-47.

[198] P. Gentile, V. Chiono, I. Carmagnola, P.V. Hatton, An overview of poly(lactic-co-glycolic) acid (PLGA)-based biomaterials for bone tissue engineering, Int. J. Mol. Sci. 15 (2014) 3640-3659.

[199] S. Das, S. Eshraghi, Mechanical and microstructural properties of polycaprolactone scaffolds with one-dimensional, two-dimensional, and three-dimensional orthogonally oriented porous architectures produced by selective laser sintering, Acta Biomater. 6 (2010) 2467-2476.

[200] S. Camarero-Espinosa, B. Rothen-Rutishauser, E.J. Foster, C. Weder, Articular cartilage: From formation to tissue engineering, Biomater Sci. 4 (2016) 734-67.

[201] J.I. Pearl, T. Ma, A.R. Irani, Z. Huang, W.H. Robinson, R.L. Smith, S.B. Goodman, Role of the toll-like receptor pathway in the recognition of orthopedic implant wear-debris particles, Biomaterials 32 (2011) 5535-5542.

[202] N. Joshi, J. Yan, S. Levy, S. Bhagchandani, K.V. Slaughter, N.E. Sherman, J. Amirault, Y. Wang, L. Riegel, X. He, T.S. Rui, M. Valic, P.K. Vemula, O.R. Miranda, O. Levy, E.M. Gravallese, A.O. Aliprantis, J. Ermann, J.M. Karp, Towards an arthritis flare-responsive drug delivery system, Nat. Commun. 9 (2018) 1275.

[203] T. Hampton, Enzyme-responsive hydrogels may help treat arthritis, JAMA 319 (2018) 2161-2162.

[204] Y.-R. Choi, K.H. Collins, J.-W. Lee, H.-J. Kang, F. Guilak, Genome engineering for osteoarthritis: From designer cells to disease-modifying drugs, Tissue Eng. Regen. Med. 16 (2019) 335-343.